EXPERIMENTAL STUDY OF MULTIPHASE FLOW OF VISCOUS OIL, GAS AND SAND IN HORIZONTAL PIPES

By

Panav Hulsurkar

A Thesis Submitted in Partial Fulfillment of the Requirements

for the Degree of

Master of Science

in

Petroleum Engineering

University of Alaska Fairbanks

May 2017

APPROVED:

Dr. Obadare Awoleke, Committee Chair
Dr. Mohabbat Ahmadi, Committee Member
Dr. Shirish Patil, Committee Member

Dr. Abhijit Dandekar, Chair
Department of Petroleum Engineering
Dr. Douglas Goering, Dean
College of Engineering and Mines
Dr. Michael Castellini,
Dean of the Graduate School

Abstract

The oil and gas industry relies on multiphase flow models and correlations to predict the behavior of fluids through wells and pipelines. Significant amount of research has been performed on the multiphase flow of different types of liquids with gases to extend the applicability of existing models to field-specific fluid conditions. Heavy oil and gas flow research commenced in the past decade and new correlations have been developed that define their flow behavior/regimes. This study aims to plant a foot in the quite deficient area of multiphase flow research that focuses on a sufficiently common situation faced by many heavy oil producing fields: the presence of sand in wells and pipelines. This study will be the first recorded attempt to understand the multiphase flow of heavy oil, gas, and sand.

A 1.5" diameter multiphase flow loop facility capable of handling solids was designed and constructed for the study. Data logging instruments were calibrated and installed to be able to withstand the erosive effects of sand. The flow loop was leak and pressure tested with water and air.

Three oils of 150, 196 and 218 cP viscosities were utilized to gather 49 single phase liquid, 227 two-phase liquid- air and 87 three-phase liquid, air and solid multiphase flow data points which included differential and absolute pressures, fluid flow rates, temperatures, liquid and composite liquid- solid hold- up data and photo and videotaping of the observed flow regimes. Validation of the setup was performed using single phase flow of oil and two-phase flow of oil and air. Sand was added in three different concentrations to the 218 cP oil and three-phase oil, gas and sand multiphase flow tests were performed.

Flow patterns were identified and flow pattern maps were created using acquired data. No change was observed on flow pattern transitions by changing oil viscosities. Liquid hold- up and differential pressures were compared to observe the effect of changing oil viscosity and the presence of sand in varying concentrations on the two-phase flow of oil and gas and the three-phase flow of oil, gas and sand respectively. An increase in differential pressures was observed with increasing viscosities and the addition of sand. No changes in hold-up were seen with changing oil viscosities rather flow patterns impacted liquid hold-up significantly. The slug flow pattern was analyzed. Composite liquid-solid hold-up in slug flow were physically measured and predicted. Liquid slug lengths were predicted and compared with observed lengths using photo

and videography techniques. Differential pressures and liquid hold-up were compared with existing multiphase flow models in the PIPESIM multiphase flow simulator to test model predictions against observed flow data. The dependence of differential pressure gradients and liquid hold-up on dimensionless variables was realized by performing normalized linear regressions to identify the most significant dimensionless groups and the results were given a mathematical form by proposing correlations for differential pressure and hold-up predictions. To the best of our knowledge, this study is the first attempt at systematically measuring pressure drop and liquid hold up during the three-phase flow of oil, gas and sand.

I dedicate this thesis to the goodwill of human beings

TABLE OF CONTENTS

Page

LIST OF FIGURES

Page

LIST OF TABLES

Page

LIST OF APPENDICES

Page

Acknowledgements

This project would not have been possible without the help and goodwill of UAF faculty, staff, students and countless early morning tech support calls.

I would like to thank Dr. Obadare Awoleke for advising and guiding me through this project. I learnt valuable lessons not only in terms of academic research, but also facing hurdles and overcoming them by sharing his stories and experiences. I greatly appreciate the financial support provided by INE and the PETE department. I am grateful to Dr. Mohabbat Ahmadi and Dr. Shirish Patil for their advice and suggestions. I am thankful to my family for being supportive throughout my graduate study program.

I cannot thank Joel Bailey enough for helping me in this project by giving me ideas, coming up with solutions and always being there to assist me. I acknowledge Paul Brown's suggestions, aid, and most importantly, his thoughts that would make me aware of all that can go wrong.

I would like to thank OJ, Gary Porter, Gary Tyndall, Wilhelm Muench, Nathan and Scott Taylor for helping me build and set up the lab, Keith Robertson III for sharing lab times and lunches, Ange, Neeraj, James, Nikhil, Aashay, Aditaya, Kushagra, Patrick, Eric, Sasha, and RJ for helping with data acquisition.

I would like to acknowledge truly empathetic employees at Continental Pumps, Cascade Machinery and Electric, Inlet Petroleum, Ferguson Plumbing, ABB, NI, who took initiatives to help me by scouting for equipment, providing valuable knowledge and information over phone calls, some of whom opted to stay past their office hours to troubleshoot equipment issues.

I also wish to thank Dr. Shirish Patil for his time he spent with me as the member of my advisory committee for this thesis. Dr. Patil was able to provide valuable assistance when needed from King Fahd University of Petroleum and Minerals (KFUPM) in Saudi Arabia, where he is now Saudi Aramco Chair Professor of Petroleum Engineering. His assistance and contributions, even though it was 12 hr difference in time zones, are highly appreciated. Also, I would like to thank KFUPM for allowing Dr. Patil to dedicate his time towards this effort while he is working there.

Chapter 1

Introduction and Literature Review

1.1 Introduction

Multiphase fluid flow studies have evolved over the past century and developed highly specific branches that investigate the effects of changing fluid properties, flow patterns or conduit orientations and shapes. Flow study of viscous oils is one of the newer areas of research. While there are a few institutions that have analyzed the two-phase flow of viscous oil and gas, there have been no reported attempts to study the effects of solids in the flow of viscous oil and gas. Sand ingress is an issue in oil and gas wells and transport facilities in Alaska and across the world and this study attempts to bridge the gap between two-phase oil and gas flow and three-phase flow, by focusing on the simultaneous flow of viscous oil, gas and sand.

Multiple old and existing flow loop facilities were studied and a small scale multiphase fluid flow loop facility was designed and setup at the University of Alaska Fairbanks (UAF). Floor design, equipment sizing and construction were the primary elements of the first phase of this project. Leak and integrity tests followed the first phase and several complications involving equipment operation and performance were overcome during the second phase. The third phase involved multiphase flow tests, data acquisition and analysis, with emphasis on slug flow.

1.2 Evolution of Multiphase Flow Studies

Multiphase flow studies have been a topic of interest in the scientific community for over a century. The oil and gas industry's lifeline are the conduits providing communication between shore/land based facilities and the subsurface; through wells. These conduits carry different phases of fluids under various flow conditions. Perhaps the first attempt to model fluid flow in wells was made by Versluys in 1930, proposing a correlation to predict pressure drop in wells. Significant assumptions were made to simplify the model as the term "Turbulence resistance" was introduced in the equations that would oppose upward flow of the fluids, in acknowledgement of the frictional losses in the tubing. In 1935, May used a generalized flow equation including friction factor equations, providing mathematical insight to Versluys' turbulence resistance idea. It was also pointed out that

frictional losses account for less than 1% of the total losses at liquid velocities of around 1 foot per second (ft/s) which were commonly observed in the Masjid-I-Sulaiman field in Iran, where this study was performed.

Traditionally, multiphase flow studies have been conducted empirically: utilizing experimental or field data to understand the changes in fluid properties under different flow conditions and to develop correlations, or mechanistically: starting with fundamental conservation of mass, energy and fluid flow equations to arrive at equations relating pressure drop or liquid hold up to fluid and conduit properties. Researchers have rarely used standalone approaches to represent their investigations. A combination of empirical and mechanistic modelling; comparing experimental data with existing models to fine- tune, or validating purely mathematical equations with observed data has engendered robust models over the years.

Different underlying assumptions form the basis of these models and they may broadly be classified into three categories: The first category groups the simplest of the models that do not consider changes in multiphase fluid flow pattern or the slippage between phases as a result of unequal in-situ phase velocities. Multiphase fluid flow studies of prominence in the oil and gas industry commenced in 1952 with Poettmann and Carpenter's pressure traverse prediction correlation, which is an example of this category of models. The authors followed an empirical approach, based on data from a large number of vertical gas lifted wells flowing at liquid rates as low as 60 barrels per day (bbl/day) to around 1500 bbl/day and Gas to Liquid Ratios (GLRs) of 5000 standard cubic feet per Stock Tank Barrel (scf/STB). They assumed fluid homogeneity. This enabled the prediction of Bottom Hole Pressures (BHPs) for determining the setting depths of Gas Lift Valves (GLVs)--a commendable achievement for that day and age. This set the ball rolling and further investigation ensued. In 1961 and 1963, Baxendell and Thomas and Fancher and Brown would make modifications to the initial model proposed by Poettmann and Carpenter in 1952, extending the applicability and accuracy of the pressure traverse prediction equations. In the late 60s, a mechanistic correlation published by Orkiszewski (1967) relaxed the underlying assumptions made by Poettmann and Carpenter on viscosity, fluid homogeneity and density to produce a more reliable correlation. This study also mentioned that slug flow is the most commonly encountered flow pattern in vertical conduits.

The second category of models considers slippage between the liquid and gas phases, owing to the difference in the in-situ velocities of liquid and gas. Hagedorn and Brown (1965) considered this effect and proposed a correlation based on dimensionless numbers to compute liquid hold-up. The dimensionless numbers used in this study were proposed by Ros (1961) in the quest to determine the optimal production string sizes and GLV installation points. The typical dimensionless analysis procedure follows the formation of dimensionless groups by identifying independent variables on the dependent variable at hand, generally pressure gradient or liquid hold-up. Using field or experimental data, the numerical values of these groups are calculated and multiple regressions are performed on these set of numbers to produce a correlation that would enable one to determine the value of the dependent variable, that is, predict pressure gradients or liquid hold-up: the core deliverable of any multiphase flow correlation. The versatility and applicability of dimensionless groups on multiphase flow research was realized around this time and was the basis for numerous multiphase flow models ever since. It still remains a widely-used approach.

The third and final category of models acknowledge the effects and changes in flow patterns as well as slippage between the phases. In 1972, Aziz and Govier concluded that empirical models based on water and air as the liquid and gas phases could not be held valid in the oil and gas industry. In 1973, Beggs and Brill published their work based on water and air flow, "A study of two-phase flow in inclined pipes", a third category model. It remains one of the most widely used models in the oil and gas industry. The authors performed an extensive literature survey before concluding that the existing correlations for pressure drop and hold-up were not robust enough to cover a wide range of fluids and/ or pipe inclinations angles. They utilized 1 and 1.5" diameter pipes, two 45ft long test sections capable of positive and negative inclinations and covered a wide range of air and water flow rates. This study was the first one to gather comprehensive experimental data that included flow rate, pressure gradient, flow visualization, inclination angle and liquid hold-up making it the first all- round study in the field of multiphase flow. Unsurprisingly, dimensionless groups were utilized to predict liquid hold- up and flow pattern transitions.

The Hasan and Kabir (1988) model is a mechanistic model from this category of multiphase flow models that consider the effect of slippage and flow pattern. Based on fluid flow mechanics, expressions were developed for flow pattern prediction, hold-up and friction factor. These

expressions were verified by testing against actual data. The convenience of this model was the simplistic and direct nature of equations, requiring fewer and less complex calculations. Several modifications were done on this model by the authors over the next decades to include the effects of pipe inclinations (1992), counter- current fluid flow (1994) and a unified model (2010).

Increasing accuracy and complexity is expected going from the first to the third category of models. Generally, empirical models have proven to be more reliable in predicting flow characteristics than purely mechanistic models.

In 1980, Taitel and Dukler used empirical data and dimensionless groups to focus on delineating flow pattern transitions in horizontal pipes. Based on their dimensionless numbers X, T, and, F, flow patterns could be predicted. This study covered flow patterns over a wide range of conduit sizes and opened a new branch of flow pattern- specific studies. This was one of the earliest studies to comprehensively document multiphase flow in horizontal conduits, an initial marker of the division of multiphase flow studies into horizontal and inclined pipe orientations. Subsequent analysis revealed a strong influence of flow patterns on the multiphase flow equations. With this revelation, the domain of fluid flow investigations became more focused. It also highlighted the segregation of multiphase fluid flow research into highly specific nodes, each one analyzing the effects of specific fluid properties, flow patterns and pipe orientations, mostly extinguishing the possibility of a single generic model that could apply to all possible multiphase fluid flows.

Heavy oil research has picked up pace over the past few decades, most notably from the University of Tulsa where studies of the flow of heavy Venezuelan crude was undertaken in the early 2000s at the Tulsa Unified Fluid Flow Projects labs. These studies focused on observing the effect of changing oil viscosities on pressure drop, liquid hold-up and flow patterns by segregating oils based on their viscosity into medium (10 to 180 cP) and high (>180 cP) viscosity oils. Heavy oil studies also commenced in Europe and China during this period which focused on specific flow patterns. Little research has been done on heavy oil flow modeling (Falcone et al. 2007), owing to the abundance and production of the more desirable light crude in the past century. At the time of thesis research, the latest study was performed by Zhao et al. in 2015 that investigated slug flow characteristics and proposed correlations to predict slug flow parameters such as slug length and hold-up. In this changing scenario and a shift towards unconventional hydrocarbon production, the

current research project attempted at planting a foot in this relatively new research area of heavy oil production, specifically the Cold Heavy Oil Production with Sand (CHOPS).

1.3 CHOPS and Heavy Oil in Alaska

In the 90s, small Canadian operating companies noticed that wells that continuously produced sand showed better oil productivity as opposed to wells with sand screens designed to avoid sand production. This produced sand was cleaned and separated for use in cement plants, road construction and related industries. These small advances and observations coupled with better lifespans and reliabilities of Progressing Cavity Pumps (PCPs) were largely responsible for the birth of The Cold Heavy Oil Production with Sand (CHOPS) process. CHOPS is an unconventional, non- thermal heavy crude oil production technique characterized by the deliberate production of reservoir sand to create additional flow channels for reservoir fluids to flow into wells. These sandstone reservoirs are highly unconsolidated, shallow hence cold, predominantly bearing viscous hydrocarbon devoid of lighter fractions. CHOPS wells have a production rate from 20 to 300 bbl/day (Han et al. 2007) with a stable sand cut of less than 1% (Cadrin 2015).

Alaska has heavy oil reserves in the tune of 24 to 33 billion barrels, most of which overly existing fields (Figure 1.1). This heavy oil is mostly produced from multilateral wells, some of which consist of horizontal sections of lengths exceeding one mile.

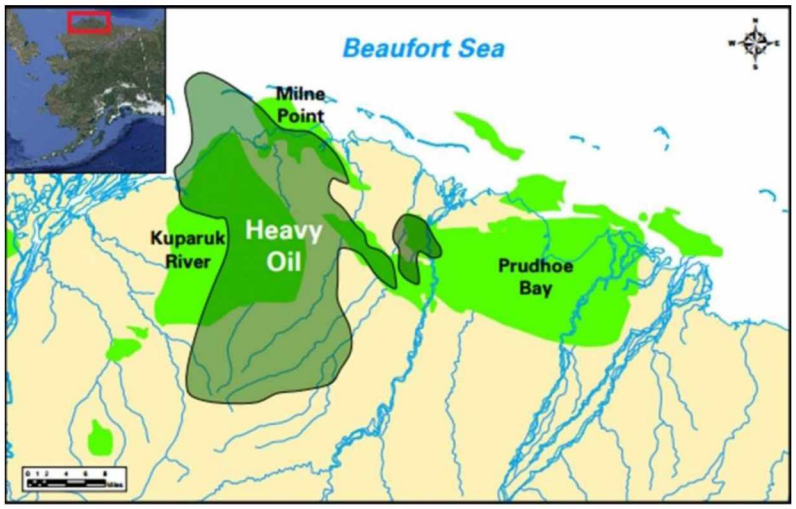

Figure 1.1: Heavy Oil fields in Alaska (Pospisil, 2011)

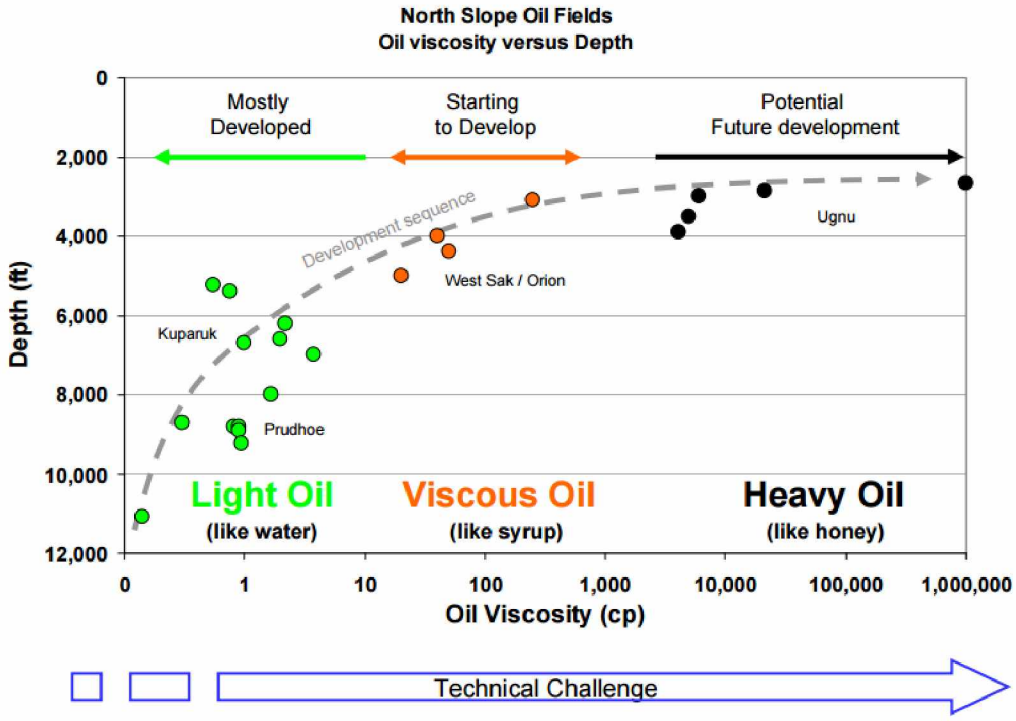

Figure 1.2: Viscosities of Alaskan Crude (Pospisil, 2011)

Milne Point, Schrader Bluff and West Sak are a few of the viscous to heavy oil producing areas, characterized by oil viscosities from the mid- teens to over 600 centipoise (cP) or 0.6 Pascal-second (Pa-s) (Figure 1.2).

Most of these wells use PCPs as an artificial lift mechanism. PCPs are screw pumps with a rotor plated with a hardening agent and a rubber stator that provide superior solids- handling performance compared the widely used centrifugal pumps in the oil and gas industry.

With no recorded attempts of studying the multiphase flow of viscous oil, gas and sand, this thesis will try to bridge the gap between the two-phase liquid- gas flow and three-phase liquid, gas and solid flow.

Chapter 2

Experimental Setup

2.1 Multiphase Flow Loop Design

Floor space in two labs on two floors of the Duckering Building was assigned for the construction of the multiphase flow loop facility. Figure 2.1 shows the floor plan on the lower and upper floors. The lower floor spanning 200ft^2 consisted of an oil tank and a PCP and the 250ft^2 upper floor housed an air compressor, a 24ft long clear test section and data logging equipment. Floor design was dependent on the load handling capacity of the grated metal floor on the upper floor of 50lb/ft^2.

2.2 Test Fluids

Industrial gear lubricating oils fit the physical properties required for this project. Phillips 66-Conoco lubricating R&O 460 oil was selected for the experiments. This oil was chosen for its low volatility and high stability over a wide range of temperatures and pressures.

Table 2.1 outlines the properties of the oil

Table 2.1: Oil Properties

Property	**Value**
Gravity (60F)	27.1 °API
Viscosity (40°C)	464 cSt (412 cP)
Pour Point	-15°C

Diesel was mixed in specific ratios with this oil to achieve different oil viscosities. Compressed air was used as the gas phase in the experiments.

2.3 Equipment

2.3.1 Oil Pump and VFD

A PCP was chosen owing to its superior solids- handling ability and a robust build. A Continental CL6 series pump was selected for use in the setup (Figure 2.2).

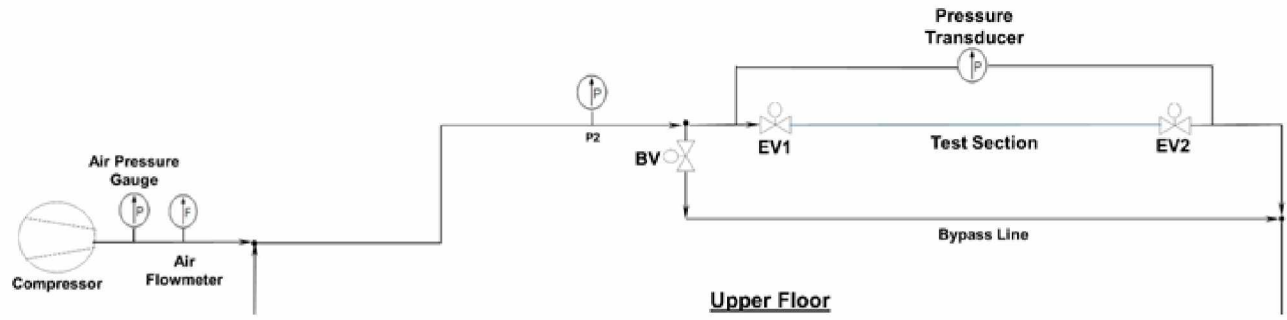

Figure 2.1 (a): Flow Loop Floor Plan: Upper Floor

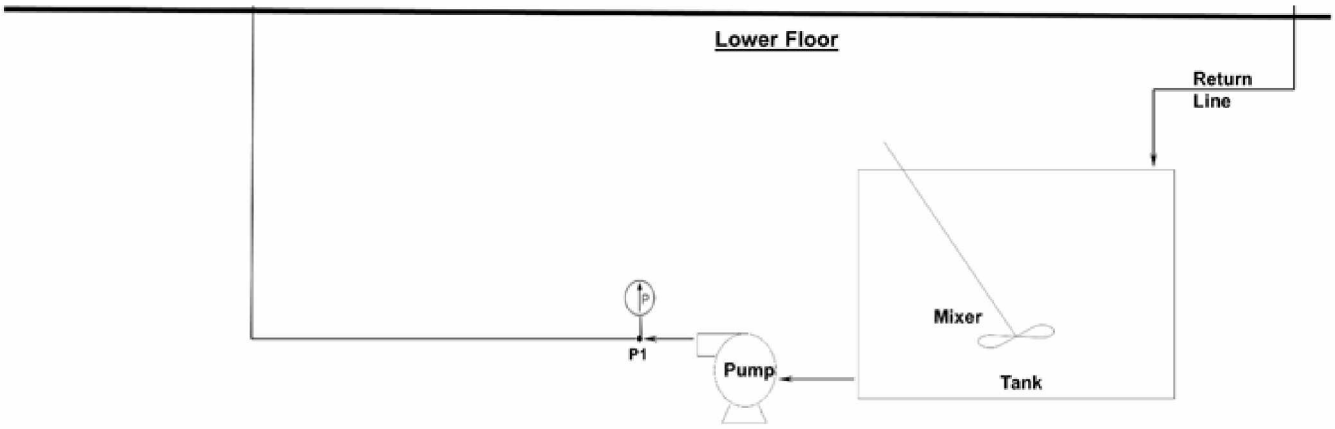

Figure 2.1 (b): Flow Loop Floor Plan: Lower Floor

Table 2.2: Floor Plan Legend

Legend	
P1	Pump Discharge Pressure Gauge
P2	Test Section Inlet Pressure Gauge
BV	Test Section Bypass Valve
EV1 and EV2	Electrically Actuated Valves

The rotor was double-lobed and chrome plated and the stator was made from heavy duty buna rubber. The pump was powered by a 7.5 Horsepower (hp) Baldor motor coupled with a gearbox. The peak pump output was 35 gallons per minute (GPM) or 850 bbl/ day at 225 psi.

Figure 2.2: Continental Progressive Cavity Pump

To control pump speeds and therefore liquid flow rates, an ABB Variable Frequency Drive (VFD) was used (Figure 2.3). The VFD could control pump speeds by supplying user- defined frequencies. Parameters such as motor rpm, torque rating, current draw, and temperature could be monitored in real time on the VFD display.

Figure 2.3: ABB Variable Frequency Drive

2.3.2 Air Compressor

A Chicago Pneumatic air compressor with an enclosed 7.5hp piston pump over an 80- gallon tank was used as a compressed air source (Figure 2.4). The compressor had a peak output of 22.3 cubic feet per minute (cfm) air (0.03 MMscf/day) at 175psi. A regulator was used to control air input to the flow loop.

Figure 2.4: Air Compressor

2.3.3 Holding Tank and Confinement

A 32 inch diameter, 5 ft tall double walled 12- gauge steel 200 gallon tank was constructed by Greer Tanks, Fairbanks (Figure 2.5). The tank outlet had an initial diameter of 1.5 inch, which was gauged up to 3 inch to match the oil pump inlet size. The tank and oil pump were enclosed within a tarp confinement as a spill control measure.

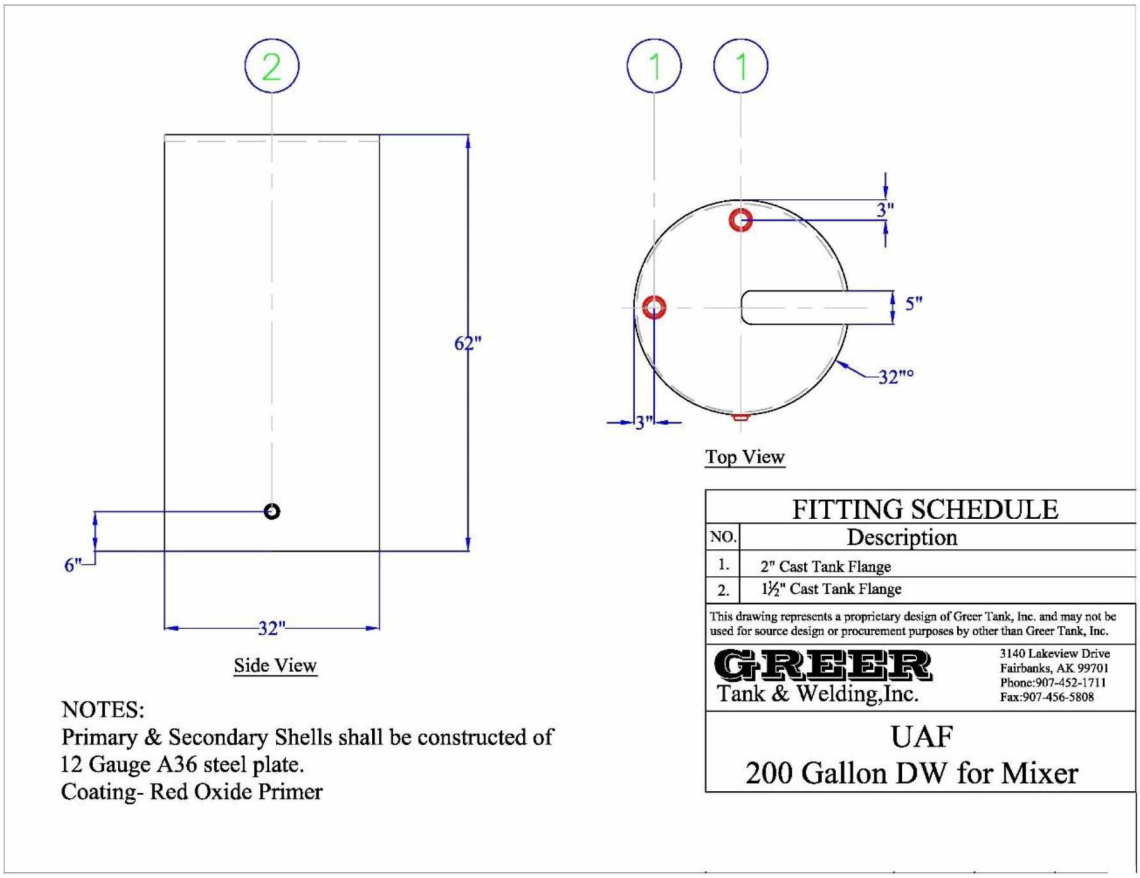

Figure 2.5: Double Walled Tank Drawing

2.3.4 Plumbing

One- and- a- half inch Schedule 80 PVC plumbing was used in the setup, manufactured by Charlotte Pipe and Foundry Company, purchased from Ferguson Plumbing, Fairbanks. The pipes were rated at 460 psi at 60 °F. All connections were made using primer and heavy duty PVC cement.

2.3.5 Measurement

2.3.5.1 Oil Flow Rate and Drive

The oil flow rates were calculated using the pump curve for the continental 3CL6 Series pump (Figure 2.6).

PERFORMANCE DATA
MODEL: 3CL6

RPM	100	300	500	700	900
NPSH REQ'D	.6	1.7	2.9	4.1	6.9
MIN. HP	1	2	3	5	5

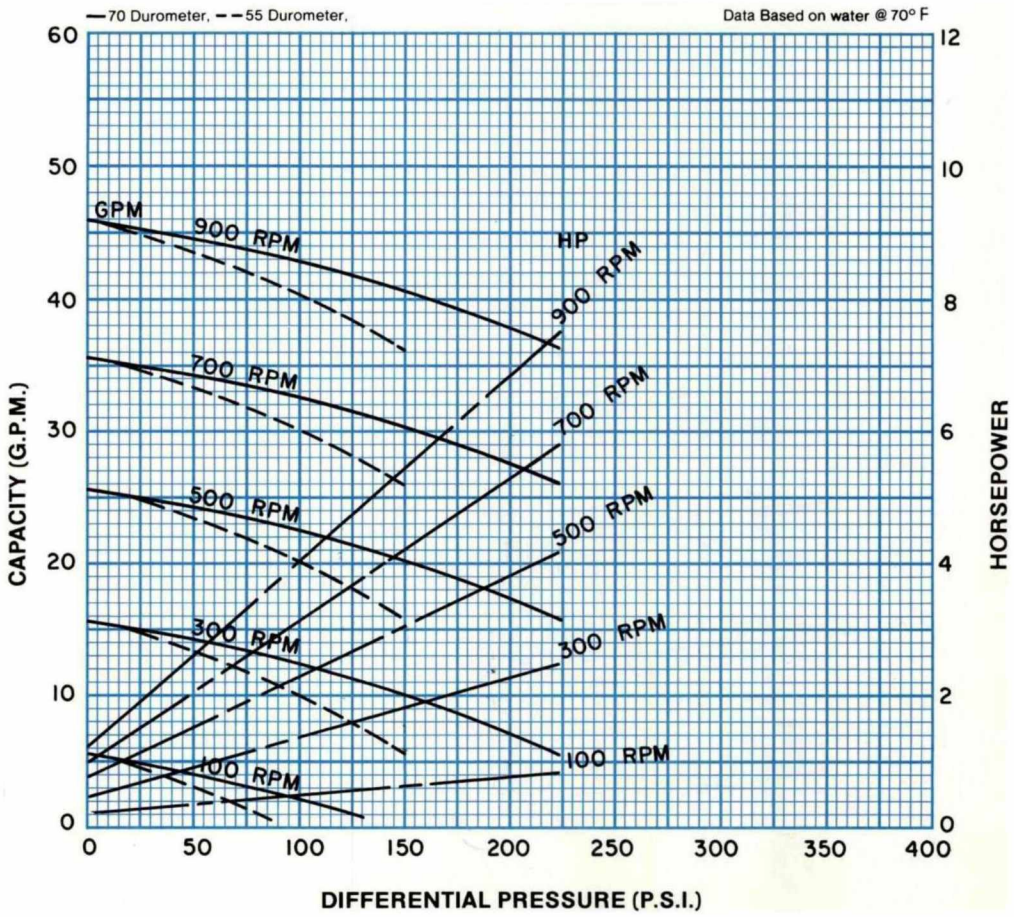

Continental Pump Company
29425 State Hwy B | Warrenton, Missouri 63383| Tel: 636-456-6006 | Fax: 636-456-4337| Email: sales@con-pump.com
www.continentalultrapumps.com

Figure 2.6: Continental 3CL6 Pump Curve

2.3.5.2 Air Flow Rate

A Cole Parmer anemometer was used in line with the air source to measure air flow rates (Figure 2.7).

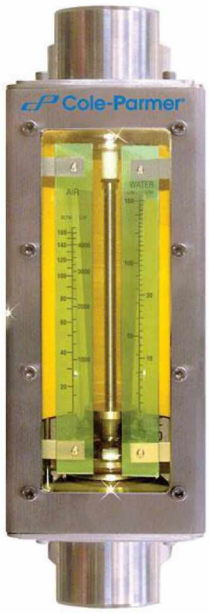

Figure 2.7: Anemometer

Figure 2.8: Differential Pressure Transducer

2.3.5.3 Differential Pressure

Foxboro pressure transmitters with protective steel diaphragms were installed at the test section (Figure 2.8) that were connected to a National Instruments' Data Logger Module 9203.

2.3.5.4 Hold-Up

To trap fluids in the test section for liquid hold-up measurements, two electrically actuated valves from Spears company were shorted and wired for synchronized operation (Figure 2.9).

2.3.5.5 Fluid Temperature

A molded Omega RTD sensor was used to measure temperature of fluids. The resistance output figures from the sensor were correlated linearly with temperatures.

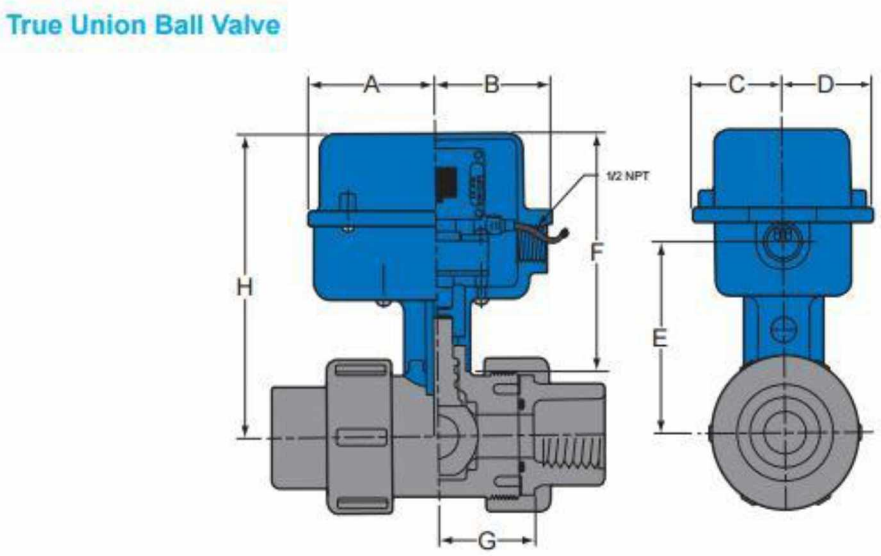

Figure 2.9: Electrically Actuated Valve Drawing

2.3.5.6 Oil Viscosity

An OFITE Model 900 viscometer was used to measure oil viscosities of different diesel- oil ratios (Figure 2.10). Three oils of 150, 197 and 218 cP were formulated with diesel-oil ratios of 1:2.8, 1:3.2 and 1:3.4 by volume for use in experiments.

Figure 2.10: OFITE Viscometer

ORCADA software was used to design viscosity tests and control the viscometer (Figure 3.11). All Diesel- Oil mixtures were categorized as Bingham Plastic fluids.

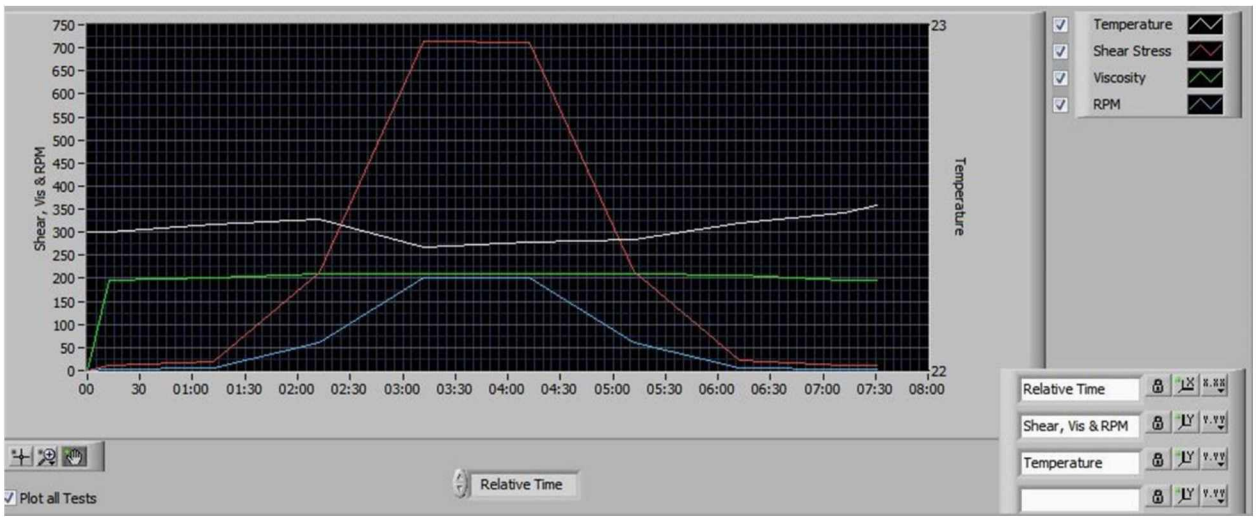

Figure 2.11: ORCADA User Interface

2.3.5.7 Surface Tension

Oil-Air Surface tension was measured using a Scientific Company Tensiometer (Figure 2.12). Average surface tension was calculated to be 29.4 dyne/cm.

Figure 2.12: Tensiometer

2.3.5.8 Sand Handling

A DynaMix DMX series industrial tank mountable mixer (Figure 2.13) was used to keep the sand suspended in oil during the three- phase flow experiments of oil, gas and sand. The mixer was powered by an electric ½ hp motor and clamped on the double walled steel holding tank.

Figure 2.13: DynaMix Mixer

To protect pressure gauges from the intrusive and erosive effects of sand, Hayward PVC Gauge Guards were installed. The gauge guards had an elastomer diaphragm to protect the pressure gauge. The void space was filled with hydraulic oil (Figure 2.14).

Figure 2.14: Pressure Gauge Coupled with a Protective Gauge Guard

2.3.5.9 Photo and Videography

A Canon DSLR and a Casio Exilim High Speed Digital Camera were used to take photos and videos with a Westcott Ice Light to provide even illumination of the clear test section for studying flow patterns.

2.4 Construction

During the first phase of design and construction of the flow loop, efficient utility of the available floor space and load handling capacity of the floors were emphasized. The PCP was anchored on the lower level and suitable plumbing support structures were built. Pipe and fittings were connected and installed using primer and heavy duty cement. The air compressor, valves, logging equipment, and test section supports were installed on the upper level. Electrically actuated valves were wired, synchronized and tested before installation. The differential pressure transducer was powered and calibrated to specifications. The data logger and LabView code were calibrated and tested. VFD issues were troubleshot and the PCP was setup. In the second phase, water was used to test the integrity of the flow loop. Multiple leaks and equipment issues were identified and fixed. Oil viscosity, pump, VFD, air flowmeter and plumbing issues diagnosed and fixed and the setup was retested. Repairs and troubleshooting proved to be the most time consuming task in this project.

2.5 Experimental Procedure

The following standard operating procedure was adhered to for performing tests. Tutorial videos on the UAF Flow Loop YouTube channel can be referenced as equipment operation guides: https://www.youtube.com/channel/UCL-UArXijxJGdg-RNevi__g

Pre- Run checks: Set oil pump torque boost and speed, check air compressor charge and valve positions at the test and bypass sections. For tests with sand, start the tank mounted mixer.

1. Start the oil pump at the pre- determined speed and monitor pump discharge pressure (P1) for surges during initial speed pick- up supplied by the torque boost. (Refer to the "How to- Oil Pump" tutorial video on the YouTube channel)
2. After pump speed stabilization, introduce air up to the pre- determined flow rate by monitoring the air flowmeter. (Refer to the "How to- Air compressor" tutorial video on the YouTube channel)
3. Start logging differential pressure on LabView. (Refer to the "How to- Data acquisition" tutorial video on the YouTube channel)
4. Log pump rpm, pump discharge pressure P1 and test section inlet pressure P2.
   If applicable, take photographs and slow motion videos.

5. For tests involving liquid hold up measurements, activate the electric valves EV1 and EV2 to trap fluids in the test section while simultaneously opening the bypass valve (BV). (Refer to the "How to- Hold-up experiments" tutorial video on the YouTube channel) Once EV1 and EV2 are completely closed, stop air supply to the loop followed by the oil pump and stop logging differential pressure.
6. To measure liquid hold-up for liquid hold-up tests, wait for the trapped fluids to settle and air bubbles to break up. Depending on the flow type, wait, ranging from 2 to 30 minutes. Measure the circumference on the pipe wetted by the liquid phase at 5 different points in the test section and obtain the average wetted length to calculate the liquid hold up.
   To physically measure composite liquid- solid hold-up, dismantle and drain the test section plumbing and swab the pipe to collect residual fluids and sand. Weigh the oil and sand mixture, separate the sand and dissolve residual oil on the sand using toluene. Allow the sand to dry completely and weigh the sand.

2.6 Data Acquisition

National Instruments' analog current input module 9203 on an NI DAq 9174 chassis was used to gather differential pressure data from the transmitter (Figure 2.15). The assembly was connected to a 12V DC source. The transmitter current output range was 4 to 20mA. The NI panel was connected to a desktop and LabView was used as an interface for logging and converting current feed from the transmitters to differential pressure. A code was designed in LabView for this purpose and was calibrated during single phase liquid flow tests (Figures 2.16 and 2.17). Differential pressure data was gathered at a rate of 0.5 data points/ second. This frequency was determined to be apt after multiple observations during test runs.

Figure 2.15: NI9203 and NI DAq 9174

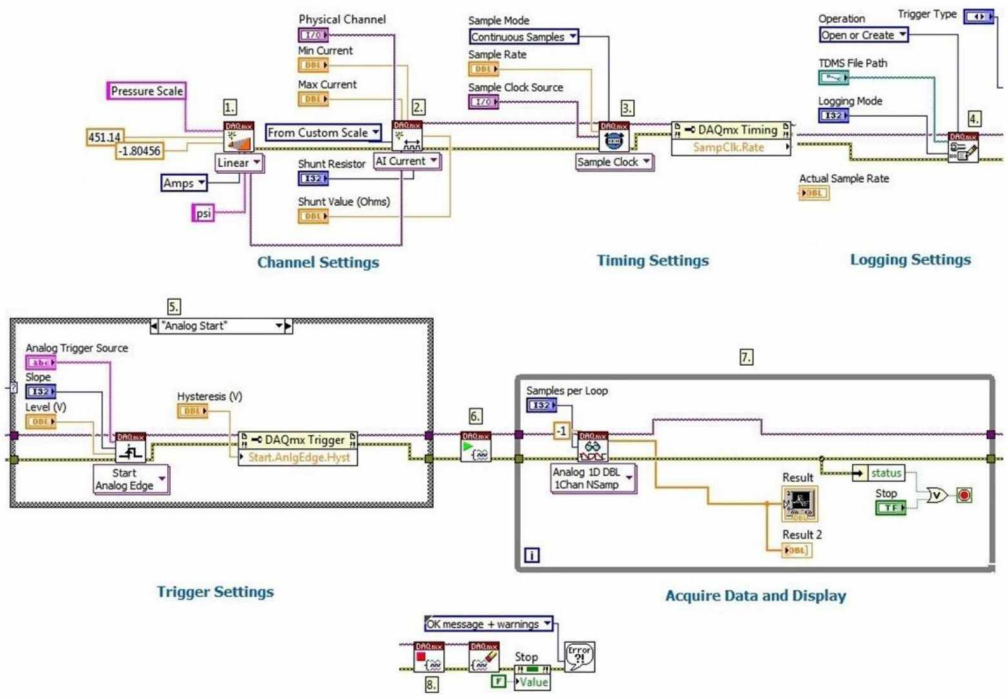

Figure 2.16 LabView Differential Pressure Logging Code

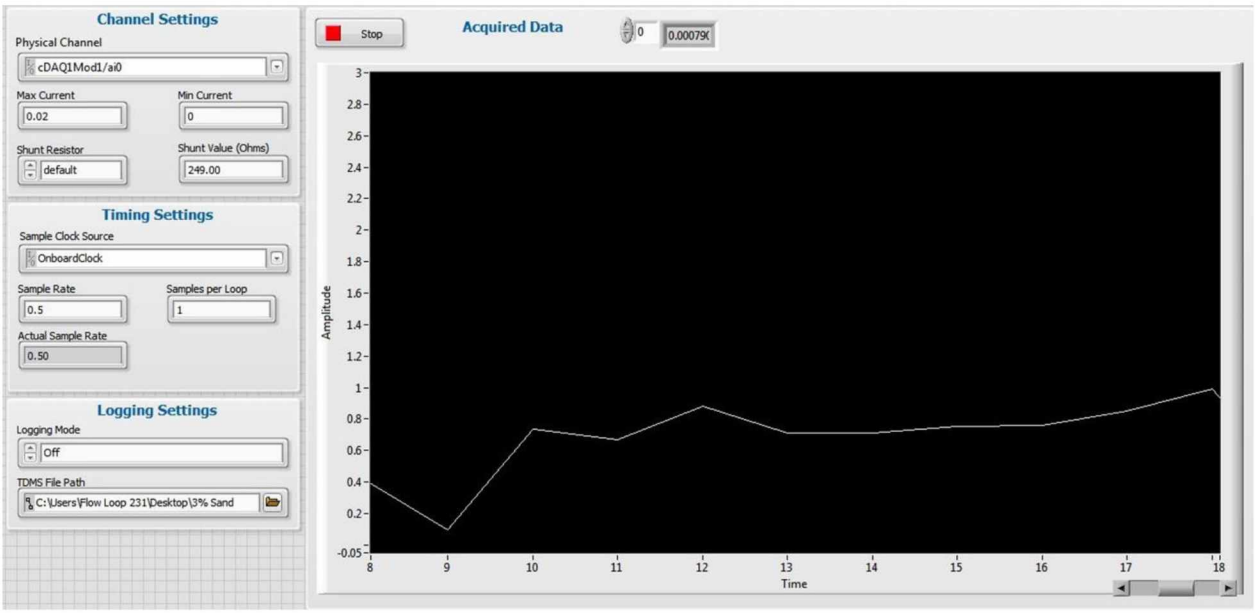

Figure 2.17: LabView Control Panel

Chapter 3

Experimental Results and Analysis

3.1 Single-Phase Oil Flow

Single phase experiments using three different oils: Diesel Mixture 1, 2, and 3 with viscosities of 149.8, 196.3 and 217.5cP at 19.9°C (0.1498, 0.1963 and 0.2175 Pa-s) respectively were carried out for validation of the flow loop. Forty-nine data points were collected for single phase flow.

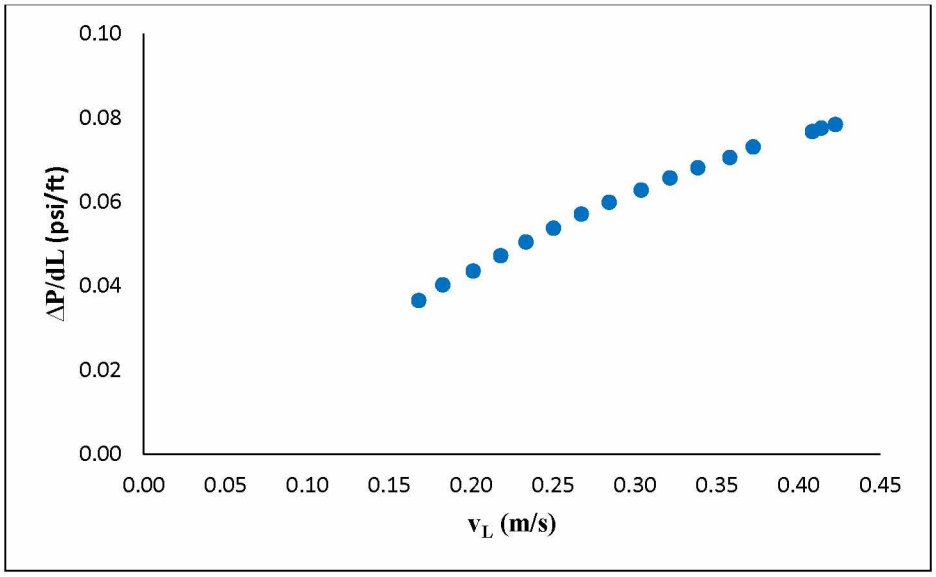

Figure 3.1: Single Phase Oil Differential Pressure Gradient, Diesel Mix 1

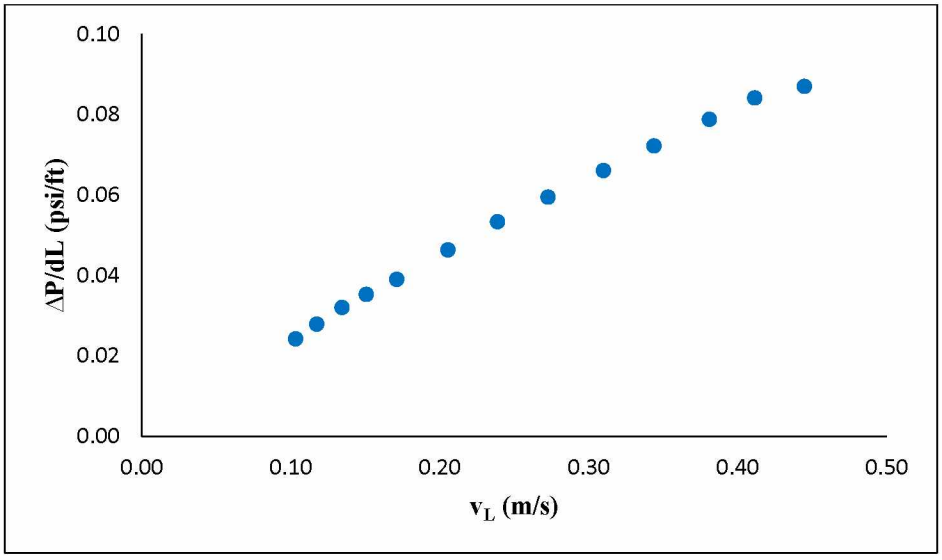

Figure 3.2: Single Phase Oil Differential Pressure Gradient, Diesel Mix 2

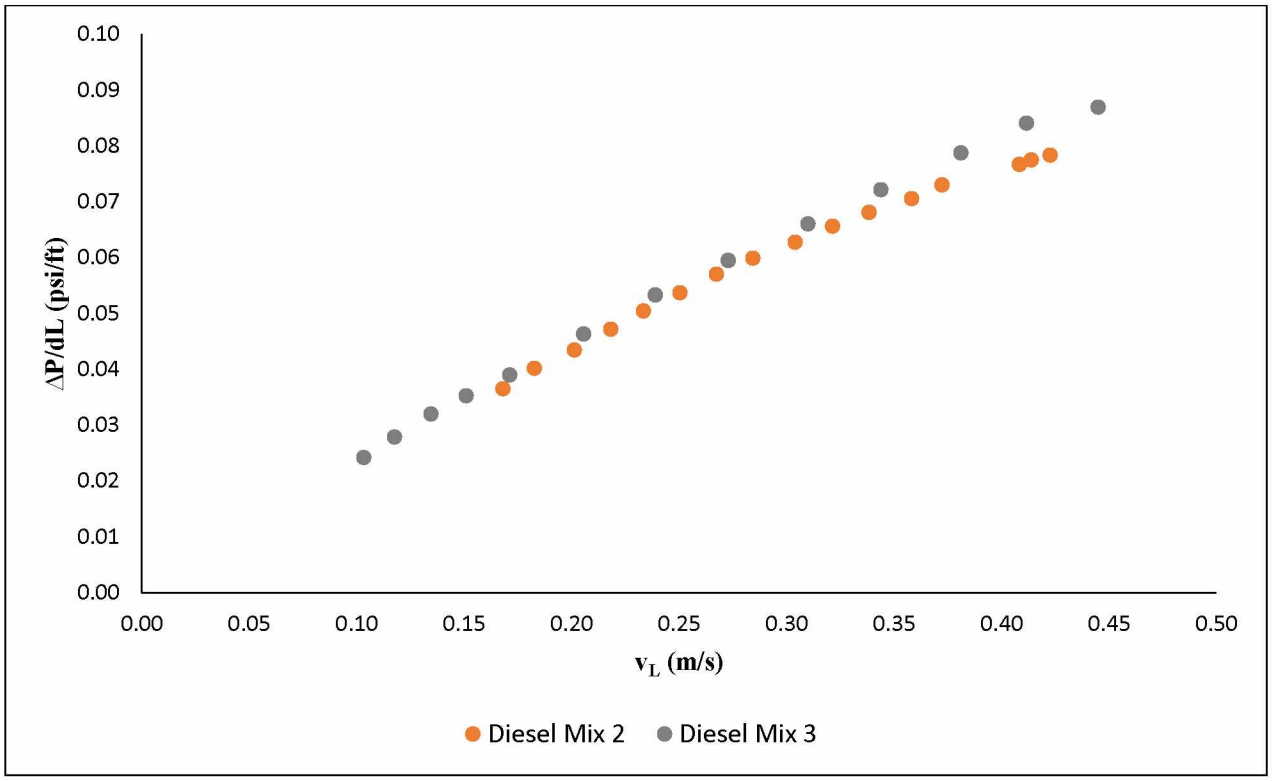

Figure 3.3: Single Phase Differential Pressure Gradient Data Comparison

Figures 3.1 and 3.2 show the differential pressure gradient for different oil velocities for Diesel Mix 1 and 2. Diesel 2 and 3 mixture pressure gradients are plotted in Figure 3.3. An increase in differential pressure was observed with increasing oil viscosities. Data for Diesel Mix 1 produced anomalously high differential pressure observations because of data logging errors.

Theoretical differential pressure equations are demonstrated in Appendix A and are plotted with observed values in Figures 3.4 and 3.5. The observed and calculated differential pressures were within close range, which gave confidence in the data quality obtained from the setup. The slight mismatch between the Bingham Plastic model with the data is accounted to the low repeatability of the viscometer in reporting yield points, which were used in calculating the theoretical pressure drop.

3.2 Two-Phase Oil and Gas Flow

The three Diesel- Oil mixtures were comingled with compressed air to analyze their two-phase flow behavior and flow patterns. Two-hundred and twenty-seven data points were collected for various oil and air superficial velocities. The data is tabulated in Appendix C.

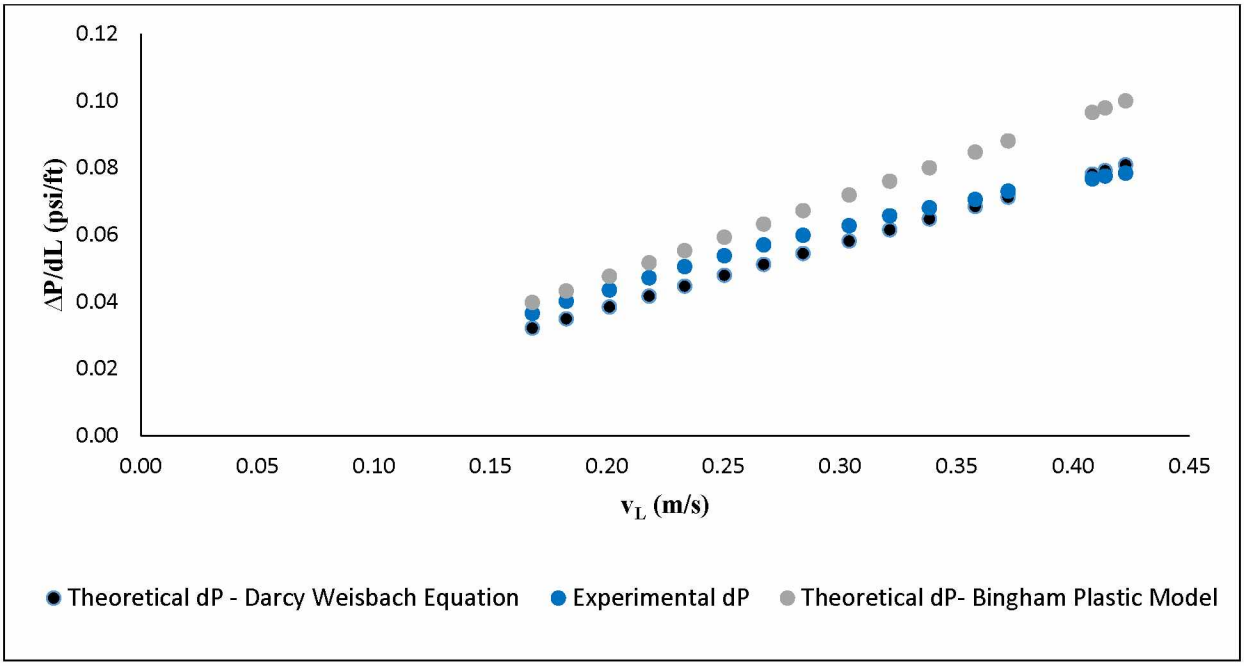

Figure 3.4: Theoretical and Observed Single Phase Differential Pressure Gradients, Diesel Mix 2

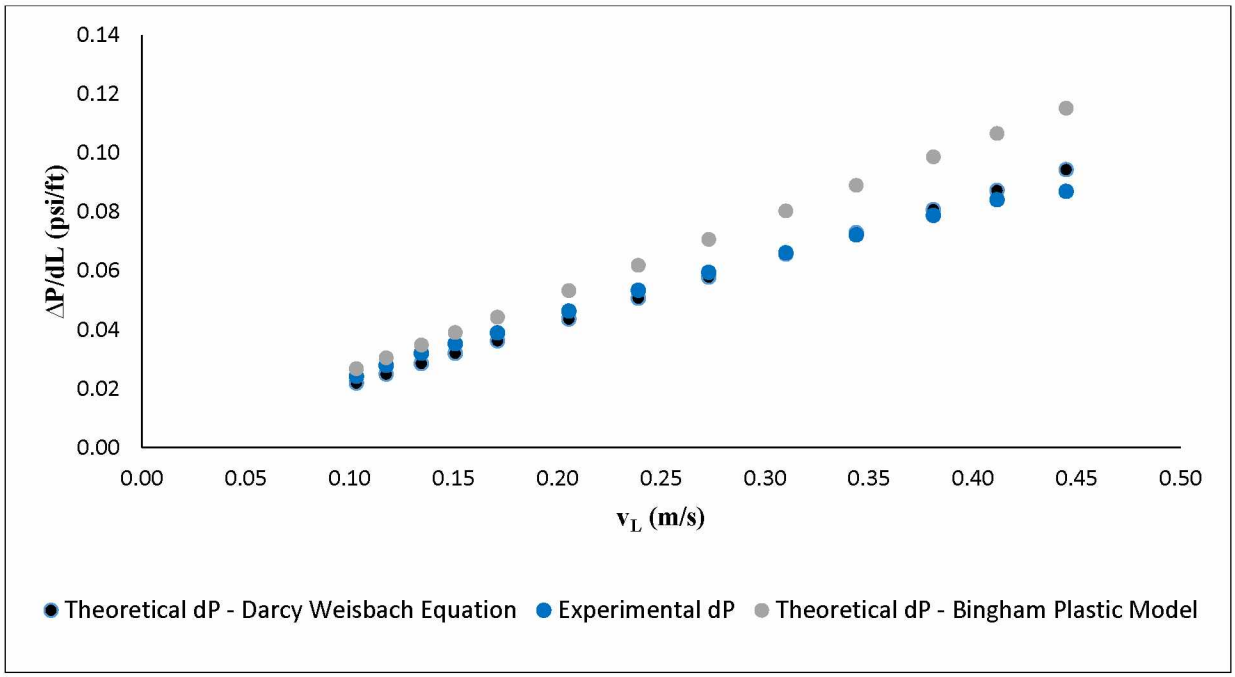

Figure 3.5: Theoretical and Observed Single Phase Differential Pressure Gradients, Diesel Mix 3

3.2.1 Flow Patterns

Six different flow patterns were observed as expected, namely, Dispersed Bubbly (DB), Stratified Smooth (SS), Elongated Bubbly (EB), Slug (SL), Annular (AN) and Stratified Wavy (SW) Flow.

3.2.1.1 Dispersed Bubbly Flow

Dispersed Bubbly flow was observed with very low gas superficial velocities at elevated oil superficial velocities, characterized by small distributed bubbles at the top of the pipe (Figure 3.6).

Figure 3.6: Dispersed Bubbly Flow (v_{SL} = 0.63m/s, v_{SG} = 0.1m/s)

3.2.1.2 Elongated Bubbly Flow

With increasing gas superficial velocities, the smaller bubbles seen in Dispersed Bubbly flow started to coalesce to form larger, elongated bubbles. Characterized by a blunt head and a wake at the rear (Figure 3.7), Elongated Bubbly flow marked the onset of intermittent flow. With increasing gas superficial velocity, the length of the elongated bubbles increased.

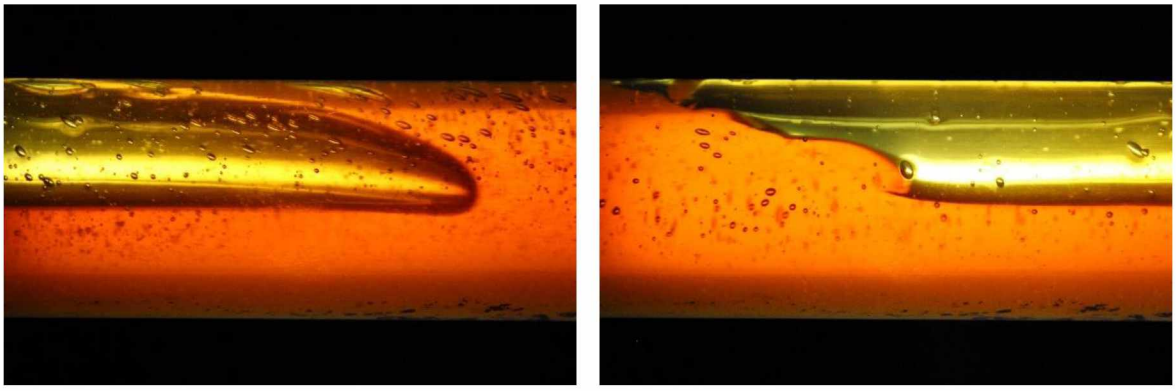

Figure 3.7: Elongated Bubbly Flow Head (L) and Tail (R) (v_{SL} = 0.27m/s, v_{SG} = 0.41m/s)

3.2.1.3 Slug Flow

The most frequently encountered flow pattern in this study was slug flow. Increasing gas superficial velocities from Elongated Bubbly flow led to the formation of slugs: alternating fast moving oil bodies separated by slower moving gas pockets with an oil film over the perimeter of the pipe. The faster moving liquid slugs appeared to engulf the oil film from the slower moving air pockets at the front, while leaving behind oil at their tails: keeping the overall slug length constant. The slug front was characterized by eddies in the front, arising from the near "bulldozing" action of the slug body on the liquid film while the tail left a liquid film behind shown in Figure 3.8.

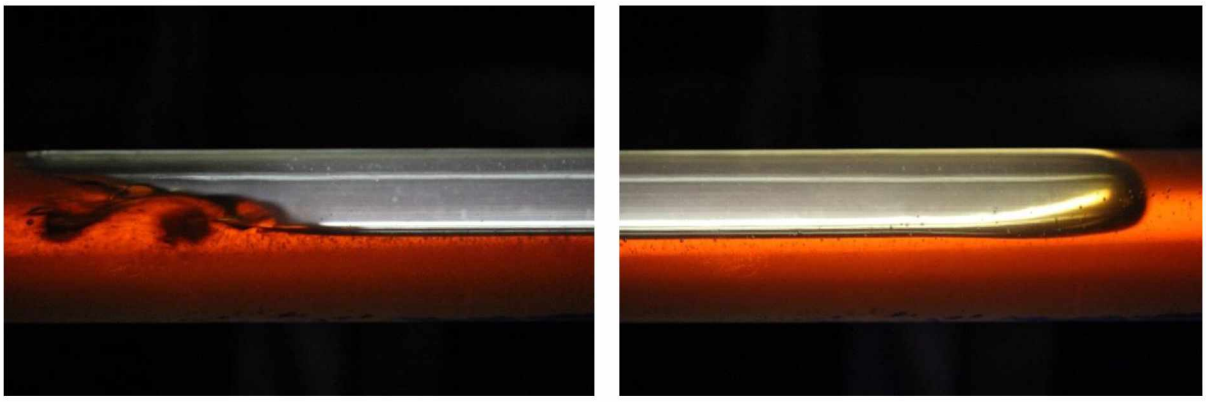

Figure 3.8: Slug Flow front (L) and tail (R) (v_{SL} = 0.27m/s, v_{SG} = 2.49m/s)

3.2.1.4 Stratified Wavy Flow

At high gas and low oil superficial velocities, the two phases flowed separately with a nearly horizontal interface. The gas phase travelled in the top section of the pipe at a much higher velocity than the oil on the bottom of the pipe, stripping oil off the gas- oil interface leading to the formation of ripples or waves on the surface of the oil in the Stratified Wavy flow pattern (Figure 3.9).

3.2.1.5 Annular Flow

The flow pattern encountered around the highest oil and gas superficial velocities was Annular Flow. The faster moving gas phase traveled through the core of the pipe, with the liquid phase flowing as a film sticking to the walls of the pipe. A higher concentration of oil was observed at the bottom of the pipe (Figure 3.10).

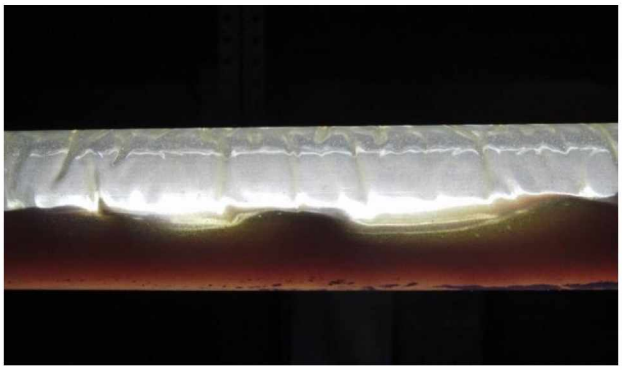

Figure 3.9: Stratified Wavy Flow (v_{SL} = 0.11m/s, v_{SG} = 5.38m/s)

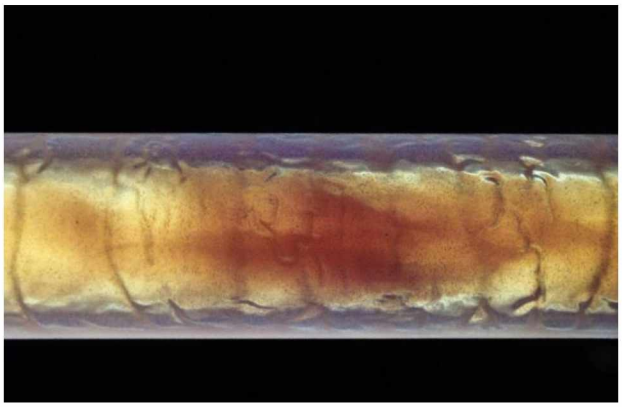

Figure 3.10: Annular Flow (Top View) (v_{SL} = 0.35m/s, v_{SG} = 9.73m/s)

3.2.1.6 Stratified Smooth Flow

Stratified Smooth Flow was observed at the minimum oil and gas flow rates. The two phases flowed independently, with the liquid phase occupying the lower part of the pipe dominated by gravitational forces (Figure 3.11).

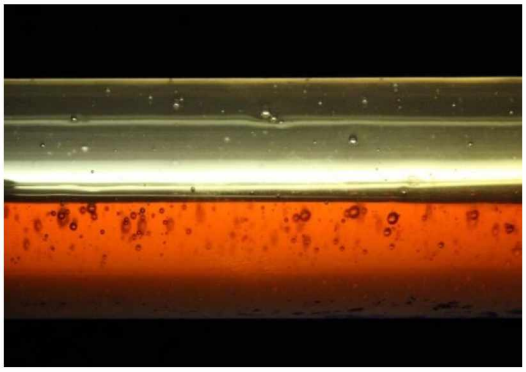

Figure 3.11: Stratified Smooth Flow (v_{SL} = 0.08m/s, v_{SG} = 0.21m/s)

3.3 Flow Pattern Map Construction and Comparison

All the observed flow patterns were plotted on a flow pattern map (Figures 3.12 through 3.14) for the three oils. No appreciable shifting of flow pattern boundaries was observed with increasing oil viscosities in the applied range.

These maps were superimposed on Taitel and Dukler's (1976) flow pattern map (Figures 3.15, 3.16, and 3.17). Some of the observed flow pattern maps data did not fit well on the Taitel and Dukler map, with majority of the points tightly concentrated between the dimensionless parameter "X" range of 10 and 100. Parameters X, K and T are detailed in Appendix B. While Taitel and Dukler's experimental scope was vast, encompassing a wide range of liquid and gas superficial velocities, the equipment in the current study was limited by the oil pump output of 0.64 to 13.6GPM (v_{SL} = 0.03 to 0.74m/s). The pump top speed was a result of the current draw limit of the motor. This resulted in concentration of data in the right half of the flow pattern map. Water was used as the liquid phase in Taitel and Dukler's study, which allows for a more ungrudging response from pumps, as opposed to viscous oil, where considerable current draw and pump speed changes are required to vary flow rates. Parameters X and K are highly dependent on liquid viscosity, which may explain the incompatibility of some of the data gathered from these experiments with Taitel and Dukler's data. Specifically, the dispersed bubbly flow regime, where the gas flow rates are extremely low which in turn led to smaller values for parameter F and a subsequent fall in the value of parameter K. This is essentially reflecting the coupled effects of high viscosity and low values of parameter F.

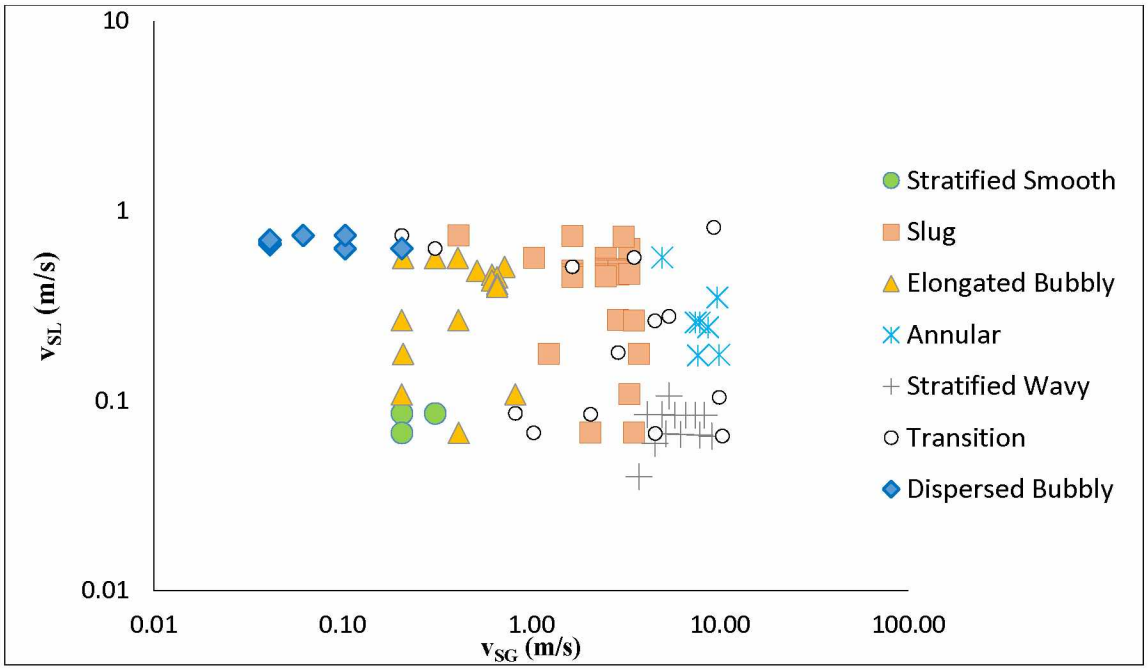

Figure 3.12: Flow Pattern Map, Diesel Mix 1

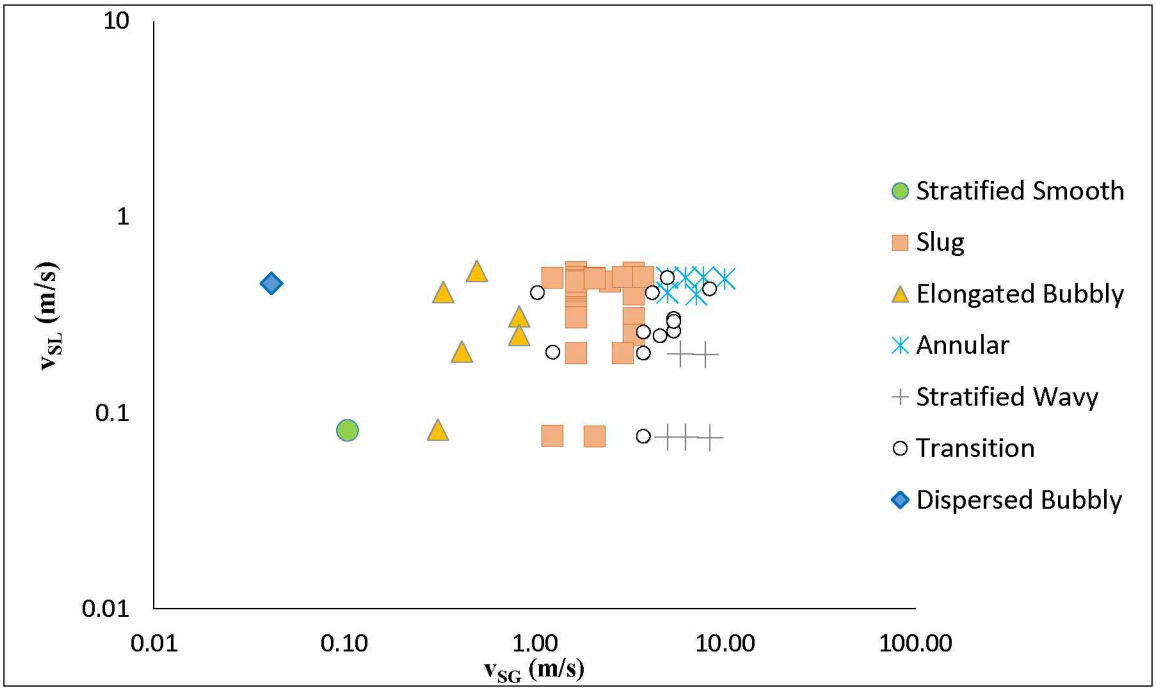

Figure 3.13: Flow Pattern Map, Diesel Mix 2

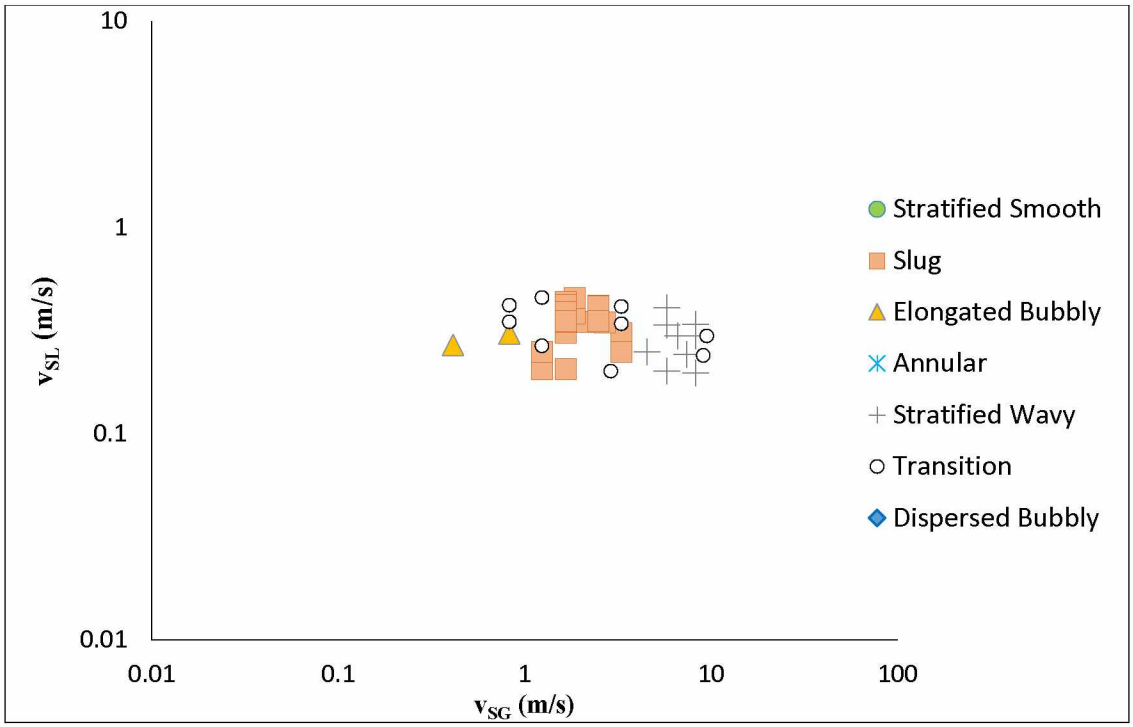

Figure 3.14: Flow Pattern Map, Diesel Mix 3

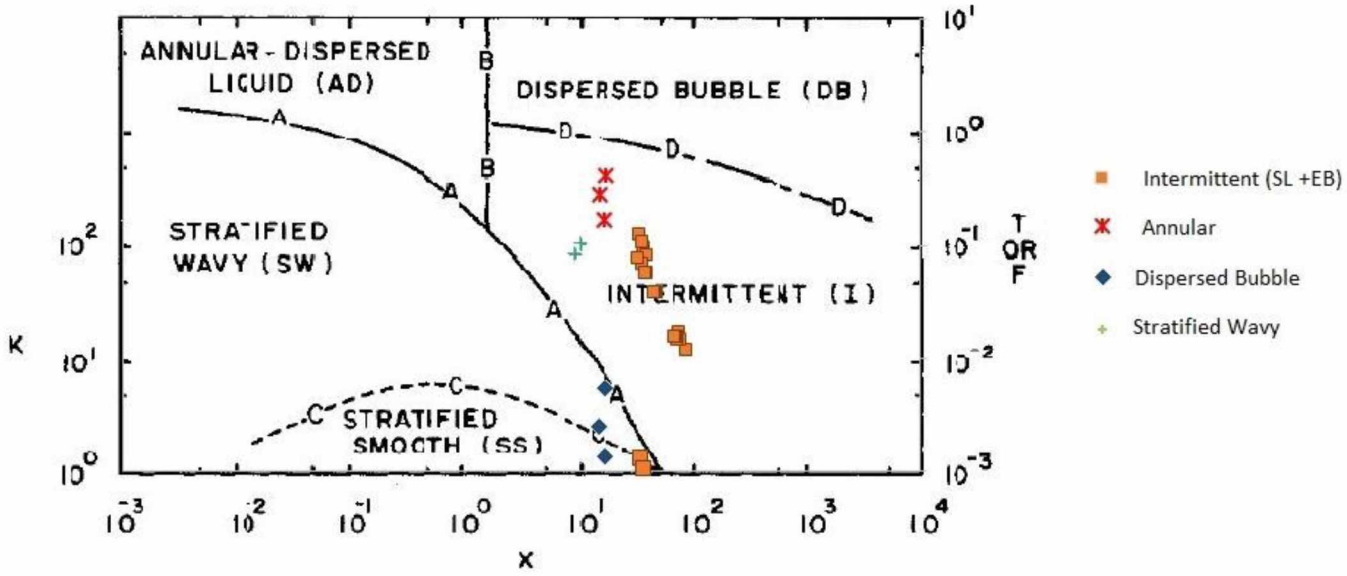

Figure 3.15: Diesel Mix 1 Two-phase data over Taitel and Dukler generalized flow pattern map

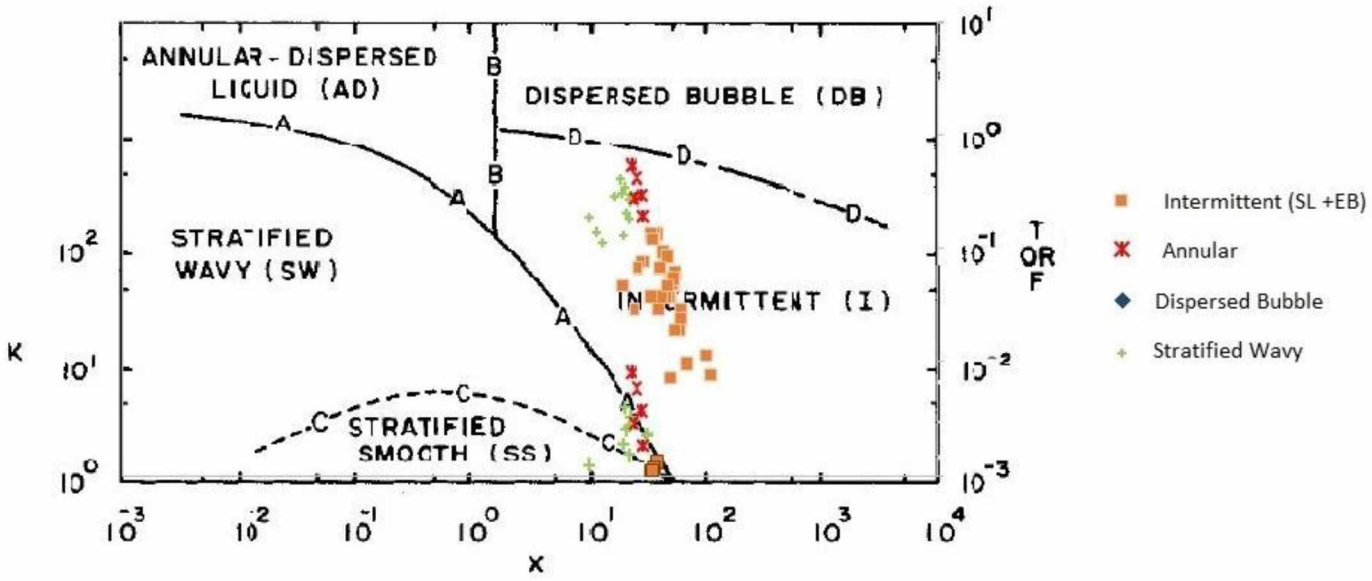

Figure 3.16: Diesel mix 2 Two-phase data over Taitel and Dukler generalized flow pattern map

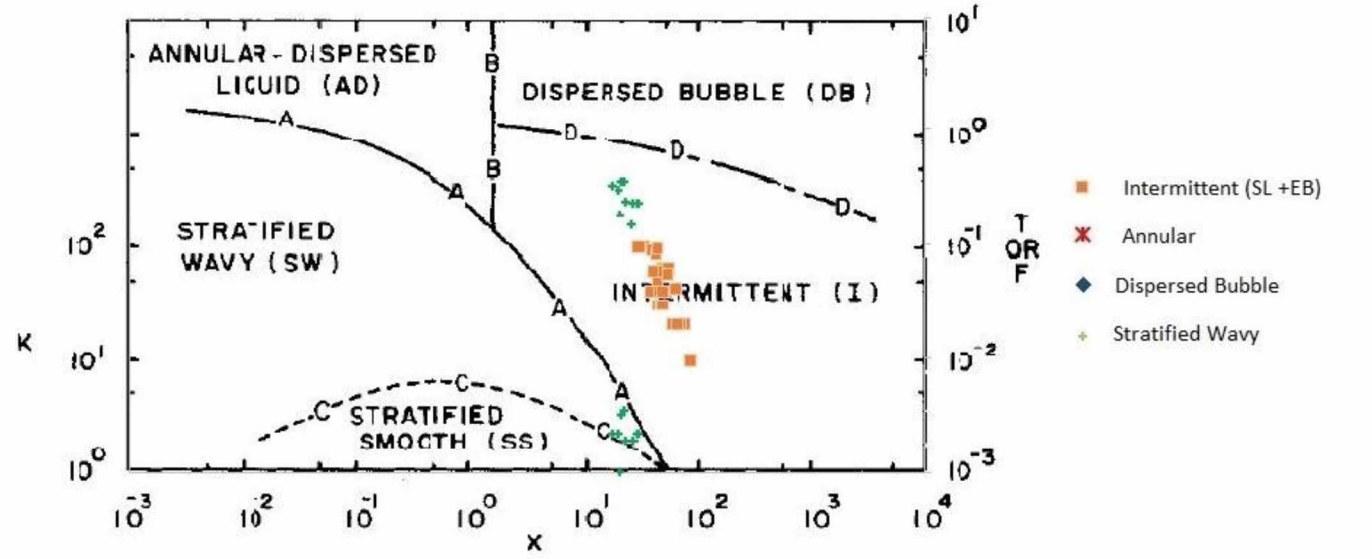

Figure 3.17: Diesel mix 3 Two-phase data over Taitel and Dukler generalized flow pattern map

3.4 Liquid Hold-Up

Eighty Liquid hold-up data points were obtained from two-phase flow of the three oils. Figures 3.18 and 3.19 show the comparison of liquid hold-up between the three oils. No significant changes were observed in liquid hold-up with changing oil viscosities. These results have also been observed by Gokcal (2005) using oil of viscosities between 180 and 580 cP. Liquid hold-up correlations proposed by Beggs and Brill (1973) and Duns and Ros (1963) consisted of empirical coefficients exclusively based on flow patterns and as stated in section 3.2, flow patterns are dominated by changes in liquid and gas superficial velocities.

Figure 3.20 shows liquid hold-up data of all the observed flow regimes on the Y axis against the number of data points for each regime on the X axis. The observed slug flow liquid hold-up was tightly knit between 0.5 and 0.6, Elongated Bubbly between 0.6 and 0.7, Stratified Wavy and Annular between 0.4 and 0.5 and Dispersed Bubbly between 0.72 and 0.9 for all two-phase flow tests of the three oils with air. These are highly specific ranges of liquid hold-up data based on flow pattern. Based on these observations, it may be hypothesized that liquid hold-up for viscous oil and gas flow is primarily a function of liquid and gas superficial velocities only.

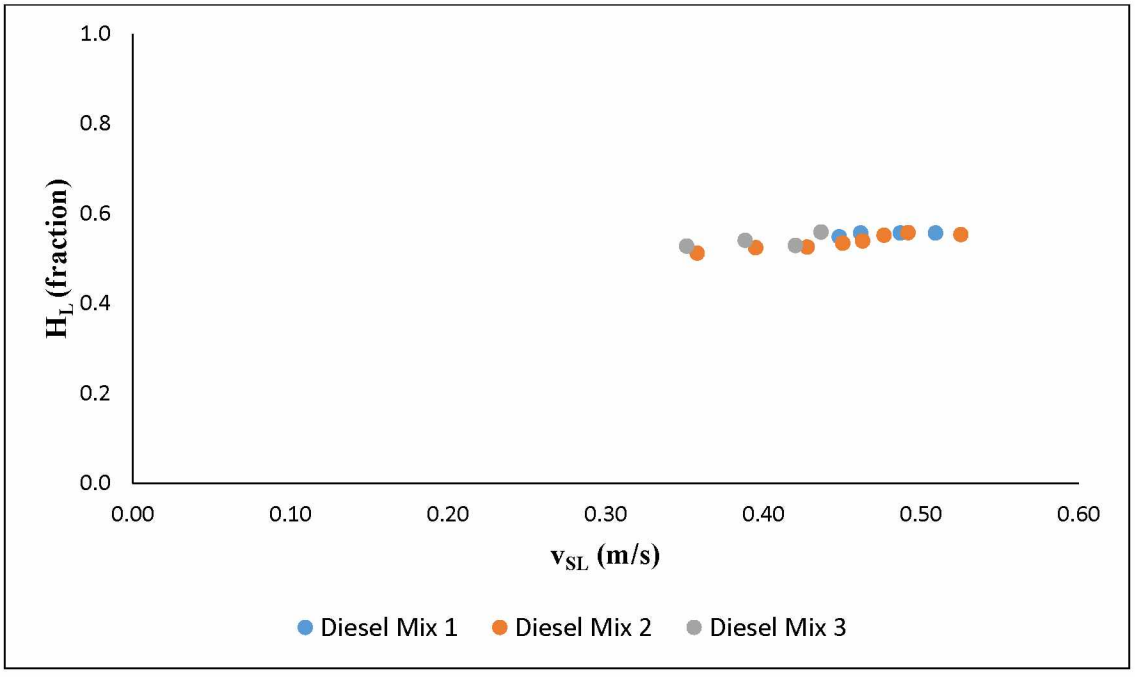

Figure 3.18: Liquid Hold up at v_{SG} = 1.66m/s

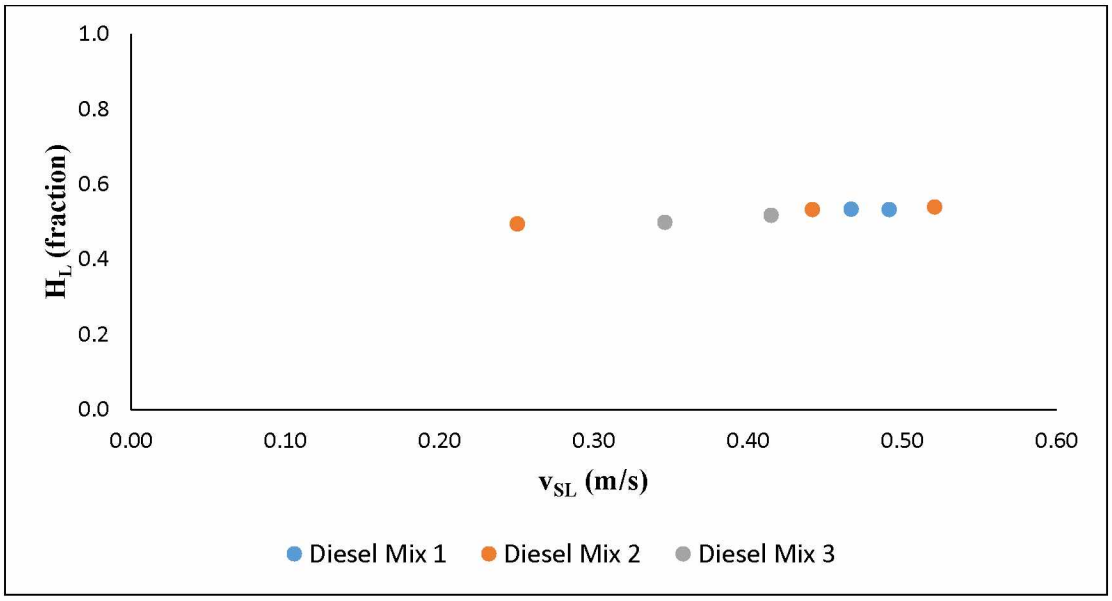

Figure 3.19: Liquid Hold up at v_{SG} = 3.31m/s

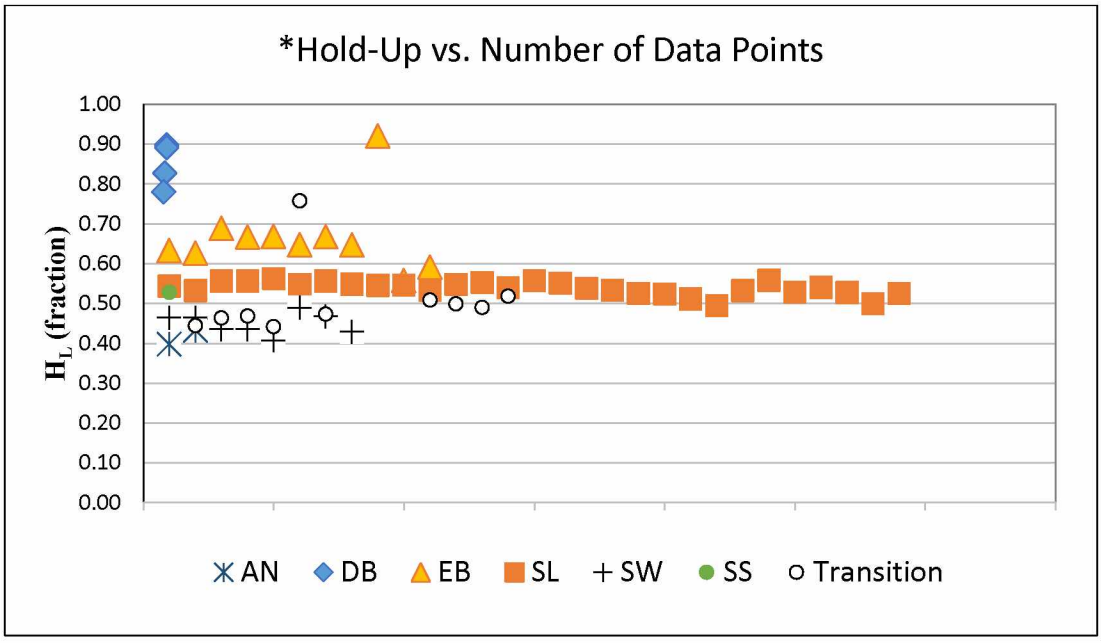

Figure 3.20: Flow Pattern Based Hold-Up

3.5 Differential Pressure

The observed differential pressure gradients for a range of different superficial oil and gas velocities for all the three oils have been plotted in Figures 3.21 through 3.25. The differential

pressure drop increased with increasing phase superficial velocities and oil viscosities. This trend has been noted by Gokcal (2005) for the study of the two-phase flow of viscous oil and gas and confirms the intuition that increased viscous drag forces will need to be overcome for increasingly viscous oils flowing at the same velocities, translating in a higher pressure drop.

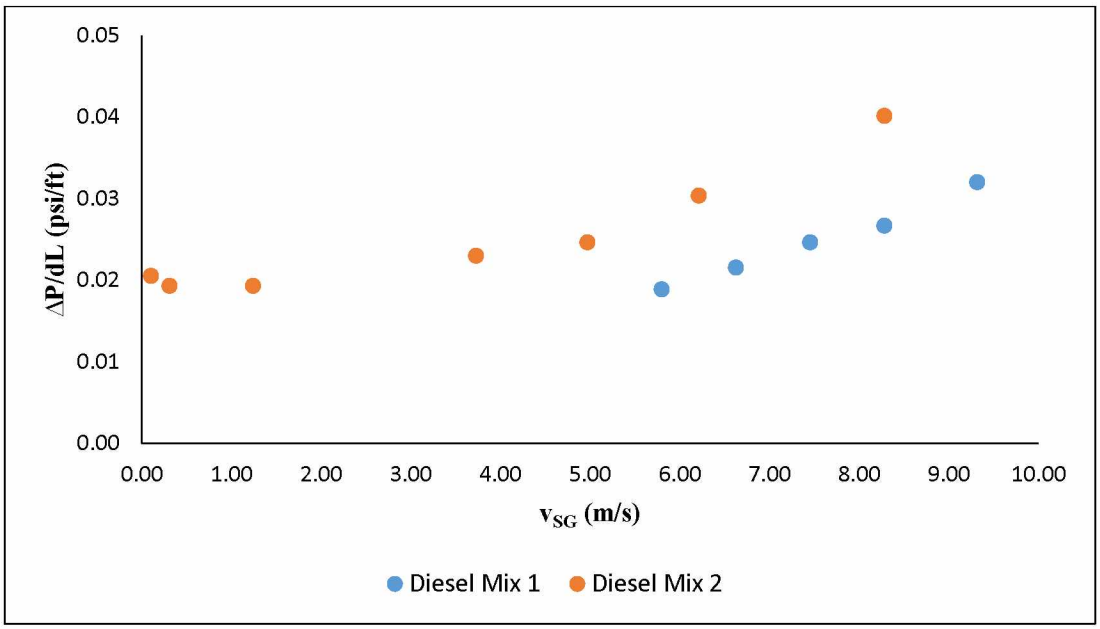

Figure 3.21: Differential Pressures, Diesel Mix 1 and 2 at v_{SL} = 0.08 m/s

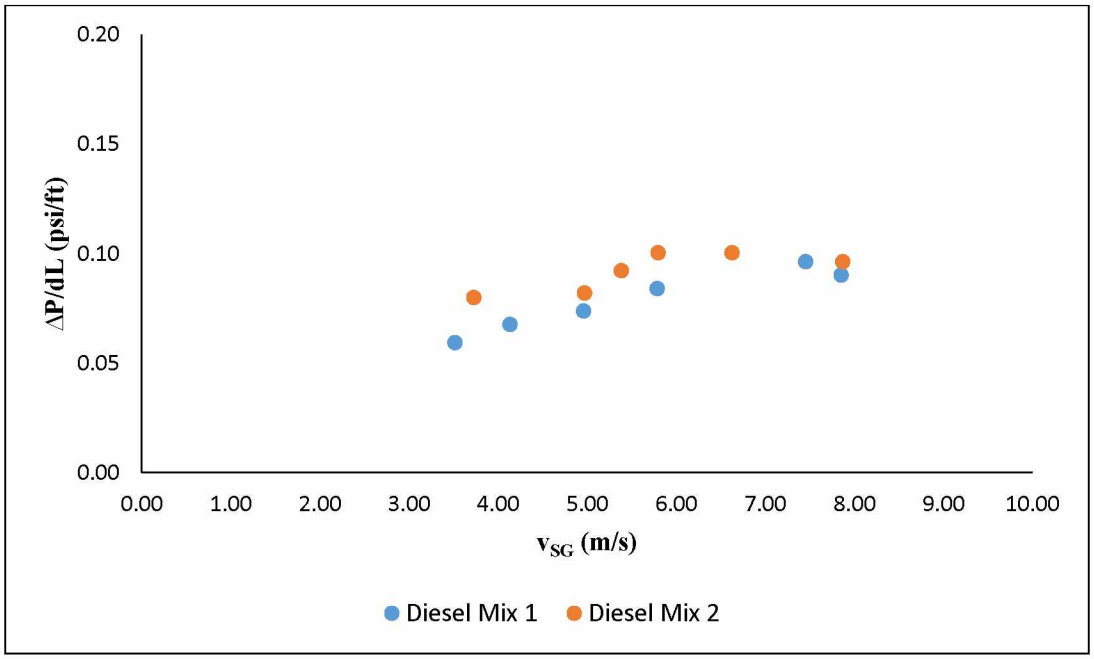

Figure 3.22: Differential Pressures, Diesel Mix 1 and 2 at v_{SL} = 0.26 m/s

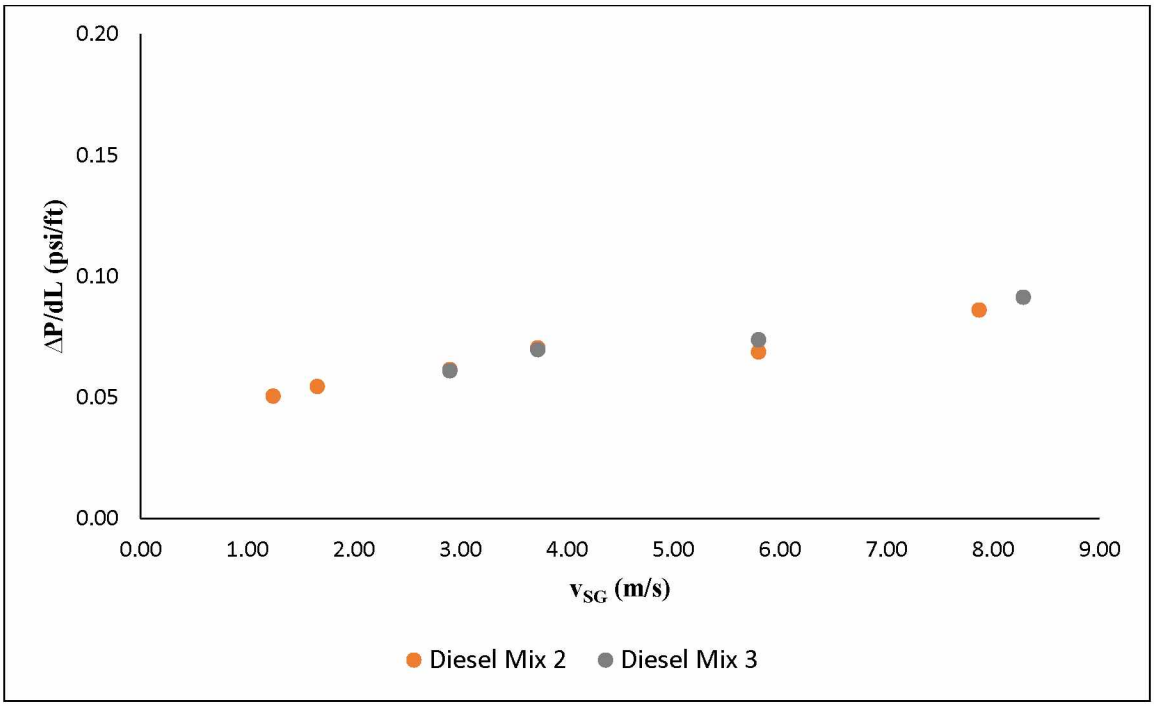

Figure 3.23: Differential Pressures, Diesel Mix 2 and 3 at v_{SL} = 0.20 m/s

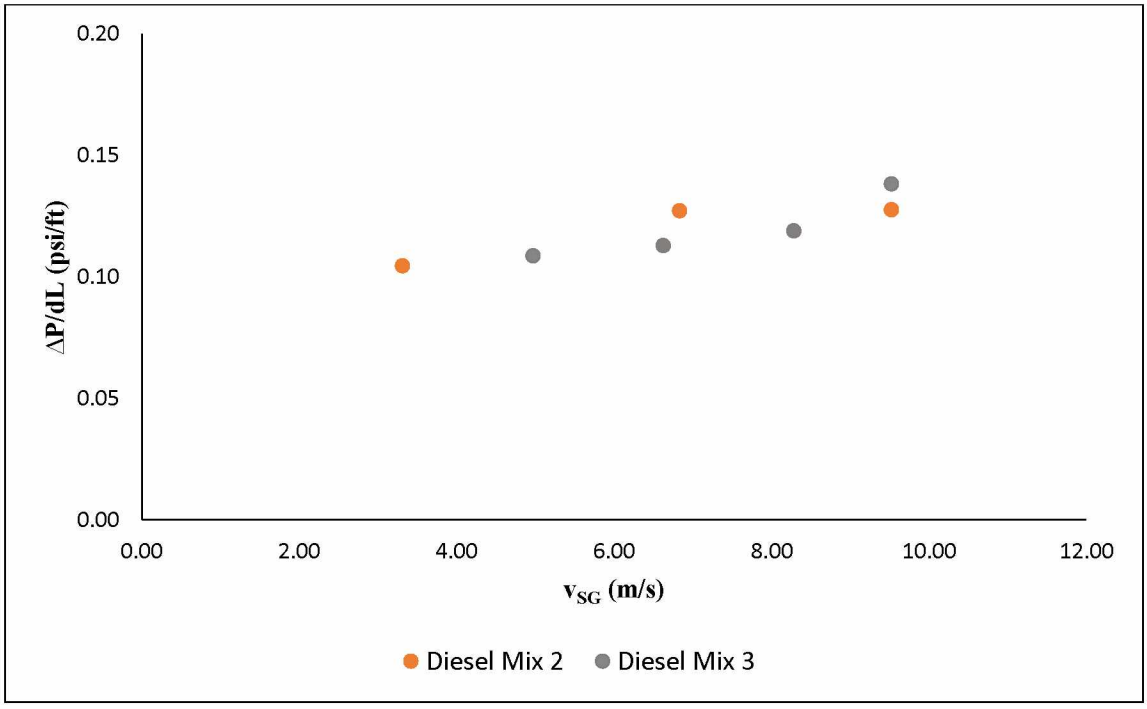

Figure 3.24: Differential Pressures, Diesel Mix 2 and 3 at v_{SL} = 0.30 m/s

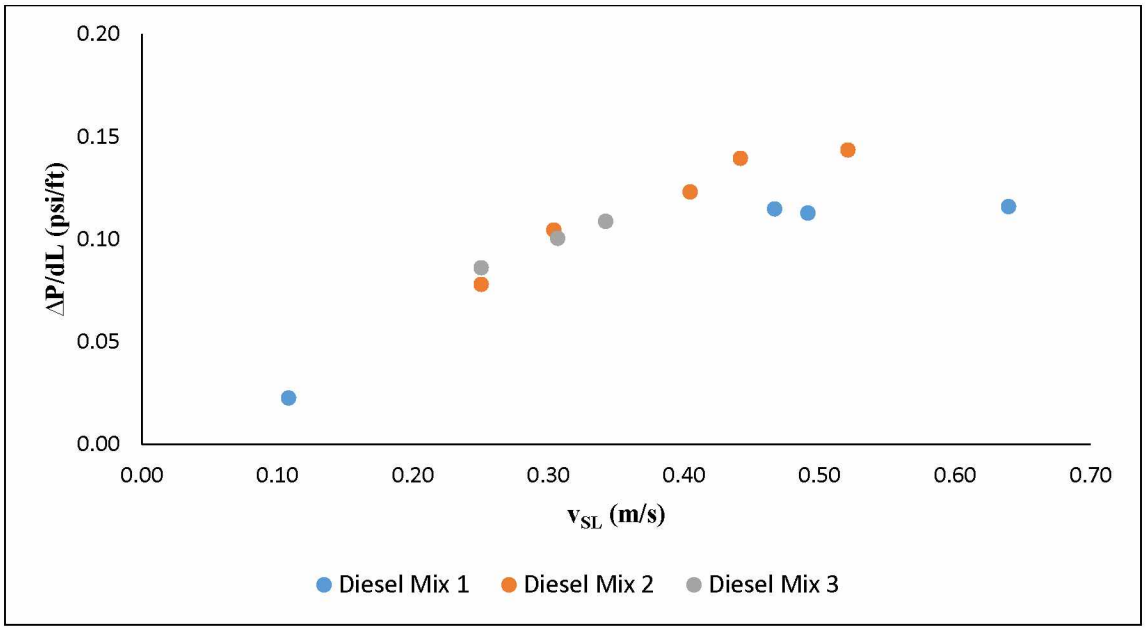

Figure 3.25: Differential Pressures, Diesel Mix 1, 2 and 3 at v_{SG} = 3.31 m/s

3.6 Multiphase Flow with Sand

3.6.1 Two-Phase Oil-Sand Flow

One percent by mass of 180μm sand was added to the most viscous oil: Diesel Mix 3, to perform two-phase oil and sand tests. This size of sand was selected because it lies close to the range of sand produced in the CHOPS process (60 to 130 μm) and due to its higher fraction in the source. A slower moving bed of sand at the bottom of the pipe was observed in the tests with faster moving suspended sand particles flowing in the rest of the pipe volume (Figure 3.26). There were some air bubbles entrained in the flow, arising from the mixing action of the impeller.

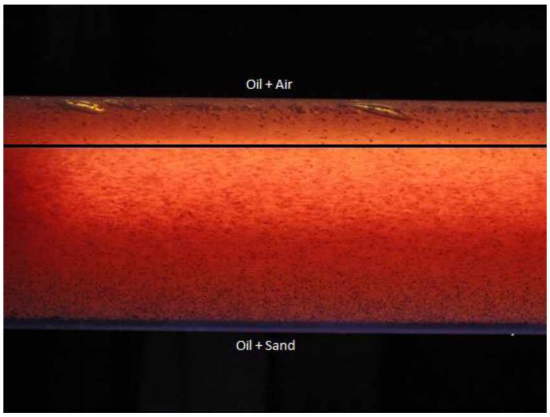

Figure 3.26: Oil and Sand Two-Phase Flow

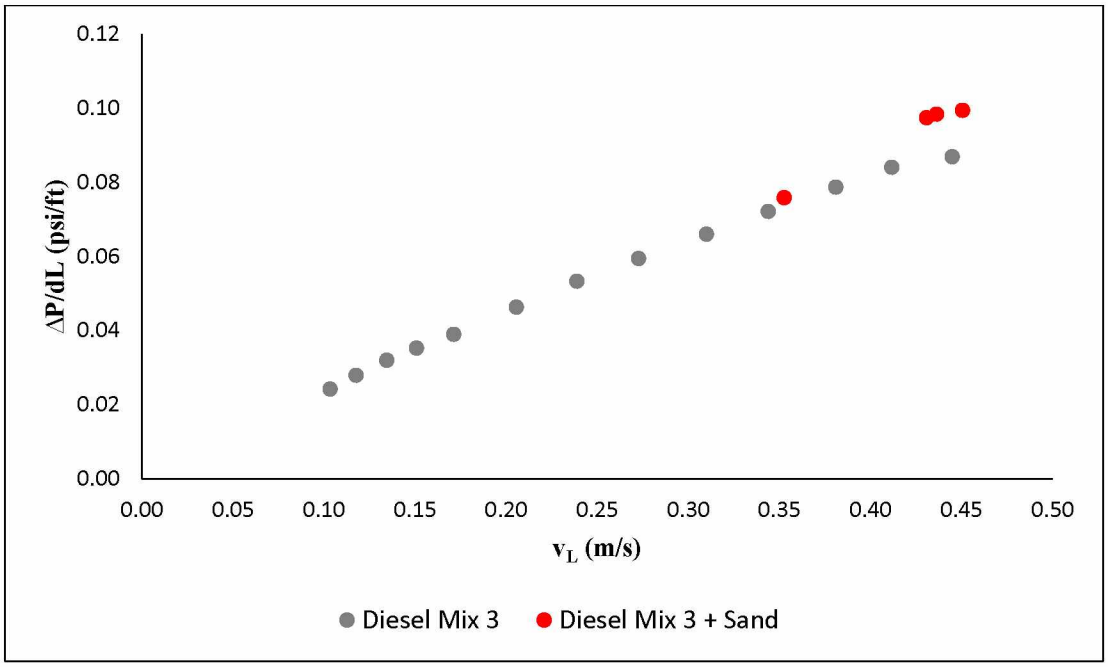

Figure 3.27: Differential Pressure Gradient, Diesel Mix 3 and Diesel Mix 3 + Sand

A higher pressure drop was observed in the two-phase flow of oil and sand. Figure 3.27 shows the increase in the differential pressure gradient of the Diesel Mix 3 and sand flow compared to the single-phase flow of Diesel Mix 3.

3.6.2 Three-Phase Oil, Gas, and Sand Flow: Flow Patterns

Three-phase oil, gas, and sand tests were performed at sand concentrations of 1, 2, and 3% and 68 data points were gathered. It is important to note here that the above sand concentrations are tank concentrations. The actual concentrations in the test section would fall below the tank concentrations and the reason why will be discussed in the following sections.

Elongated Bubbly, Slug, Stratified Wavy, and Annular Flow patterns were observed.

3.6.2.1 Elongated Bubbly Flow

The bubbles in the Elongated Bubbly flow lost sharpness at the head with more chaotic tails at the back. This effect may be attributed to the disturbances caused by the sand particles in the flow (Figures 3.28 and 3.29).

3.6.2.2 Slug Flow

With slug flow dominating the flow pattern map area, this flow regime was of particular interest in the context of sand particle transport.

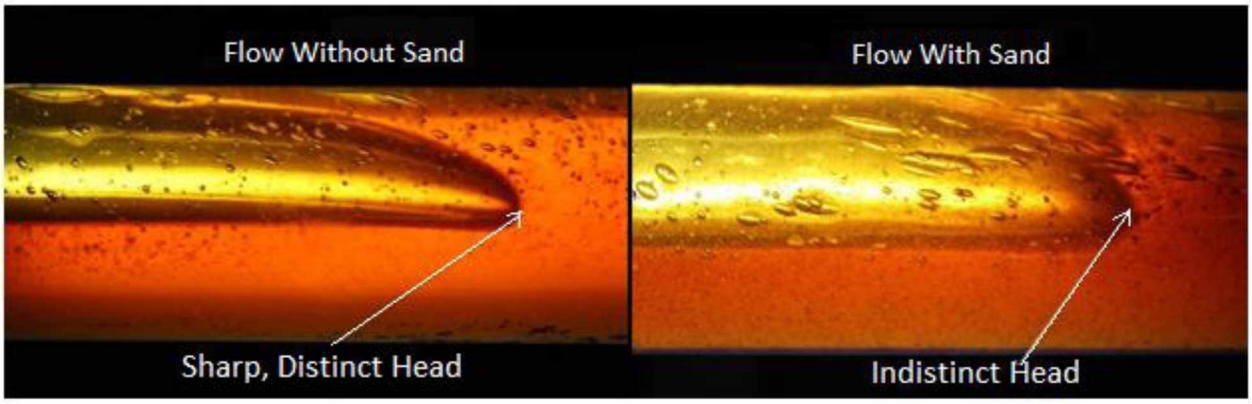

Figure 3.28: Elongated Bubby Flow Head without sand (L) and with sand (R)

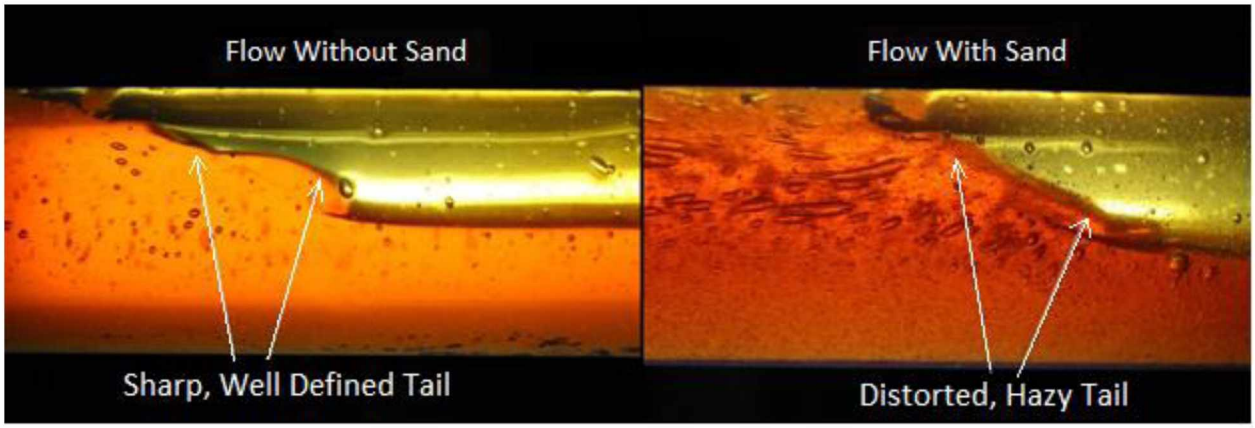

Figure 3.29: Elongated Bubby Flow Tail without sand (L) and with sand (R)

The two-phase slug flow is characterized by turbulent eddies at the front that engulfs oil from the pipe walls into the slug body and a tail at the back that leaves behind an oil film. There was a noticeable change during three-phase flow in this flow pattern. Sand was transported in two distinct motions along the pipe. The particles suspended in the slug body moved at a higher velocity than the moving bed of sand. As the slugs advanced in the pipe, they appeared to sweep the moving bed of the sand. Turbulent eddies in the wake of the liquid slugs were not as clearly distinguishable

in slug flow with sand and sand at the tail appeared to strip the liquid film from the walls on the pipe (Figures 3.30 and 3.31).

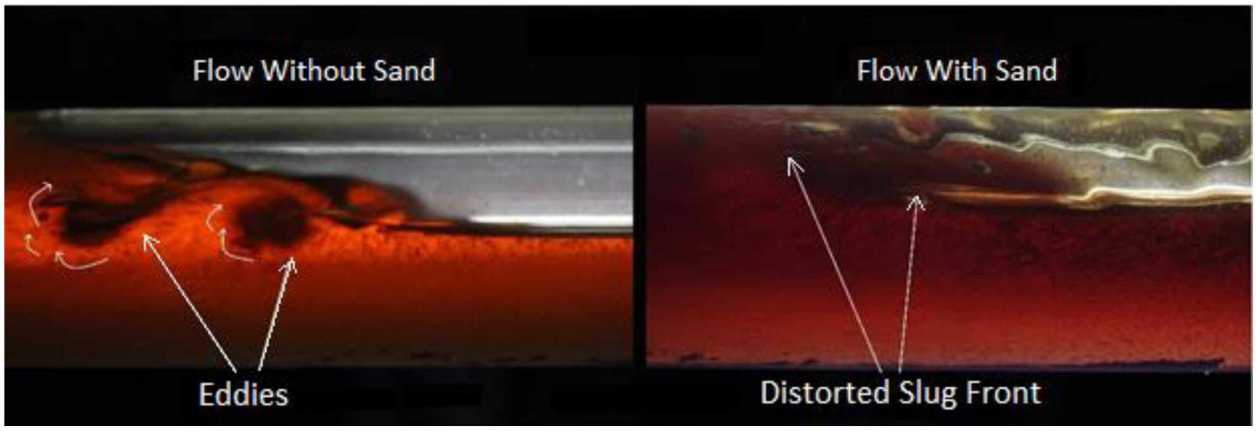

Figure 3.30: Slug Flow head without sand (L) and with sand (R)

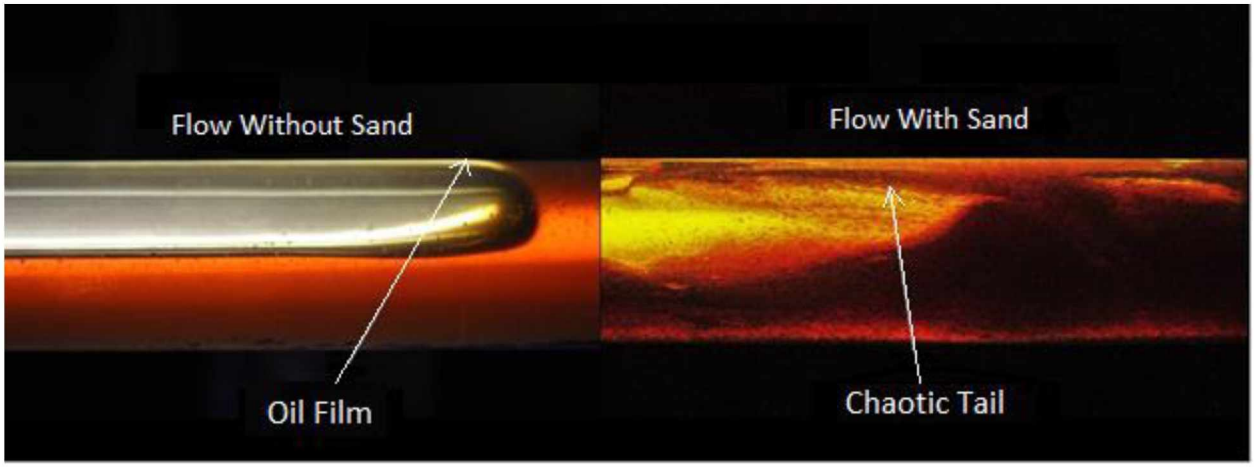

Figure 3.31: Slug Flow Tail without sand (L) and with sand (R)

3.6.2.3 Stratified Wavy and Annular Flow

Stratified Wavy Flow was encountered at high oil and gas superficial velocities, with no observable change in flow behavior in the presence of sand with the available photo and videography equipment. Annular Flow was observed at higher oil superficial velocities than Stratified Wavy

flow. The sand particles appeared to be entrained in the liquid film around the inner walls of the pipe with a higher concentration observed at the bottom of the pipe (Figure 3.32).

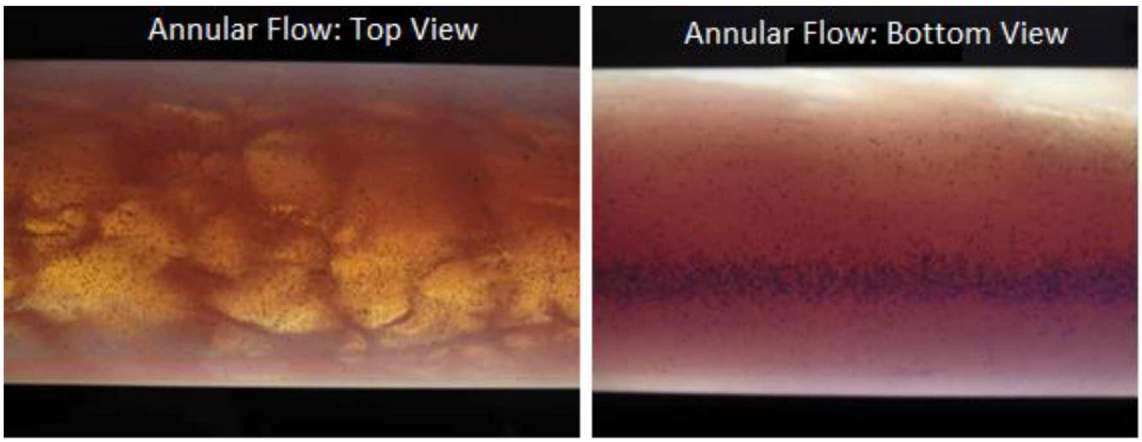

Figure 3.32: Annular Flow Top view (L) and Bottom View (R)

3.6.3 Three-Phase Oil, Gas and Sand Flow: Composite Liquid-Solid Hold-Up

Eighteen composite solid- liquid hold-up tests were performed with the three-phase flow of oil, gas and sand with 1, 2 and 3% sand concentrations in the oil tank, which are similar to the sand concentrations observed in typical CHOPS wells (Cadrin 2015) and favorable to this experimental setup. Comparing with the two-phase liquid hold-up, no significant change was observed in the liquid- solid hold-up values even with different sand concentrations in the flow. Table 3.1 contains oil and air superficial velocities and composite liquid- solid hold-up for data points 1 through 4 in Figure 3.33. Figure 3.33 shows a comparison of liquid hold-up from Diesel Mix 3 experiments and composite liquid- solid hold-up from experiments with different concentrations of sand.

Table 3.1: Superficial Velocities and Hold-Up observations

Data Point	v_{SL} (m/s)	v_{SG} (m/s)	Hold-Up			
			Mix 3	1%	2%	3%
1	0.35	3.31	0.5	0.51	0.51	0.54
2	0.35	0.83	0.55	0.57	0.56	0.57
3	0.35	2.48	0.53	0.53	0.54	0.54
4	0.41	2.48	0.5	0.55	0.54	0.55

*Data Point 1: v_{SL} for 2% = 0.34m/s, *Data Point 2: v_{SL} for 3% = 0.36m/s

*Data Point 3: v_{SL} for 2% = 0.36m/s, *Data Point 4: v_{SL} for 2% and 3% = 0.42m/s

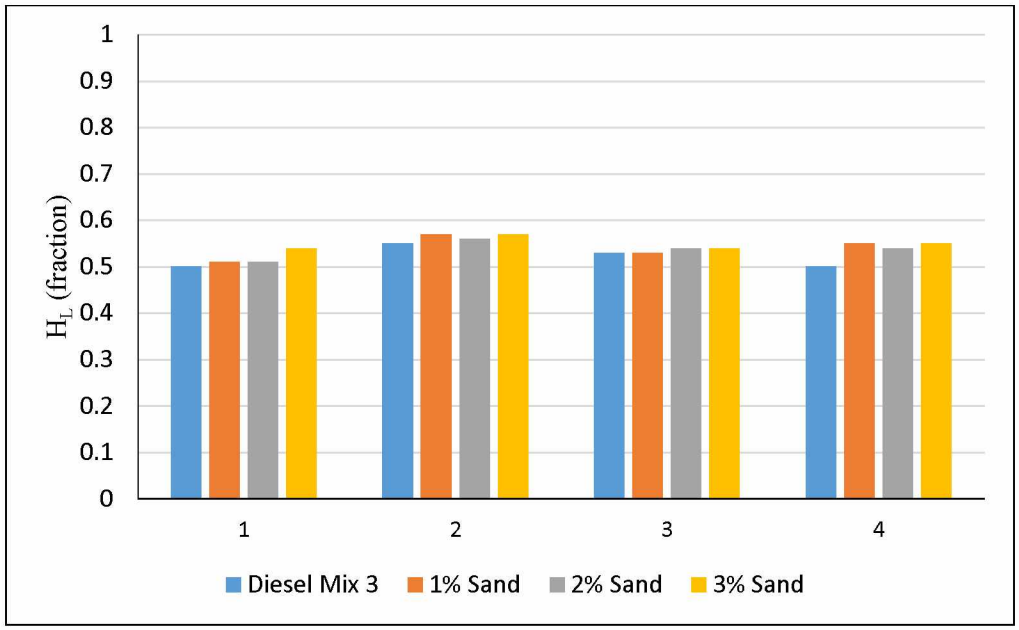

Figure 3.33: Hold-Up Comparison

The industrial mixer was not entirely effective in suspending the sand particles in the oil tank, hence there was an uncertainty associated with the actual amount of sand in the test section. A decision was made to correlate the input sand concentration and the sand concentration in the test section. To achieve this, 9 experiments were performed for the two-phase flow of oil and sand, with input sand concentrations of 1, 2 and 3% at 3 pump speeds to observe the effect of changing input sand concentrations and increasing pump speeds on the sand cut, and 3 more, to measure sand cut from the composite liquid-solid hold-up experiments.

Oil flowing at three different speeds (0.27, 0.37 and 0.42m/s) with 1% sand input concentration was trapped in the test section. The test section was drained and the oil and sand were separated to be weighed. The collected sand was then washed in toluene was used to dissolve the oil sticking to the sand particles. The sand was dried and weighed to understand the relationship between the input sand concentrations and test section sand concentrations. Similar experiments were performed with 2 and 3% input sand concentrations. Fig 3.34 shows the plot of the measured sand concentrations in the test section with 1, 2 and 3% input tank concentrations and changing oil velocities. A near-linear relationship between the oil flowrate and sand concentration in the test section was observed.

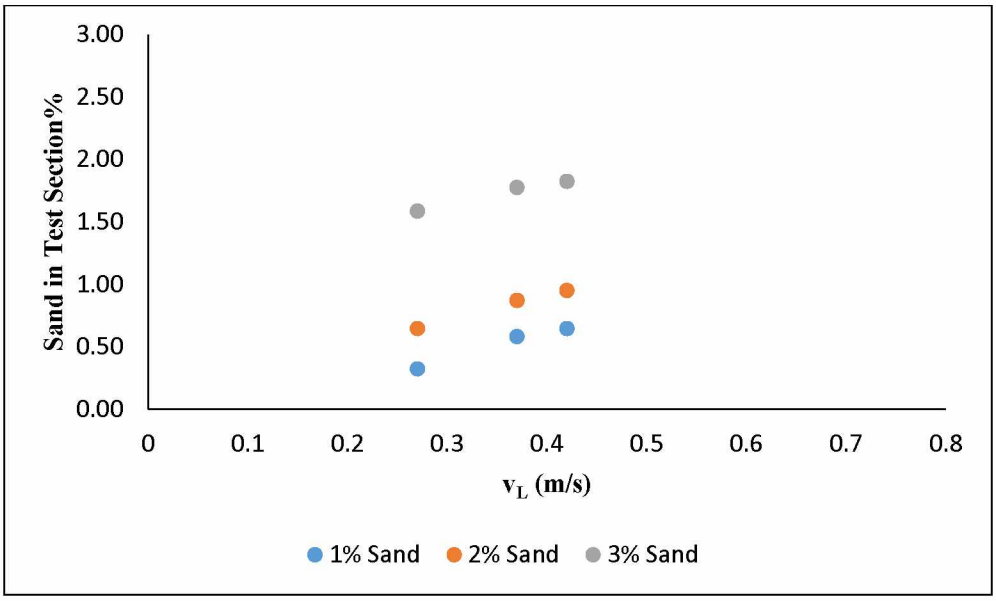

Figure 3.34: Sand cut in Test Section vs Oil Velocity

A similar approach was followed to measure the sand cut in the three-phase flow of oil, gas and sand. Three different sand input concentrations of 1, 2 and 3% under identical oil and air flow conditions were trapped and physically measured using the same approach as stated in the previous paragraph. There was a linear increase in the sand concentration in the test section with increasing input sand concentrations in the oil tank, depicted in Figure 3.35.

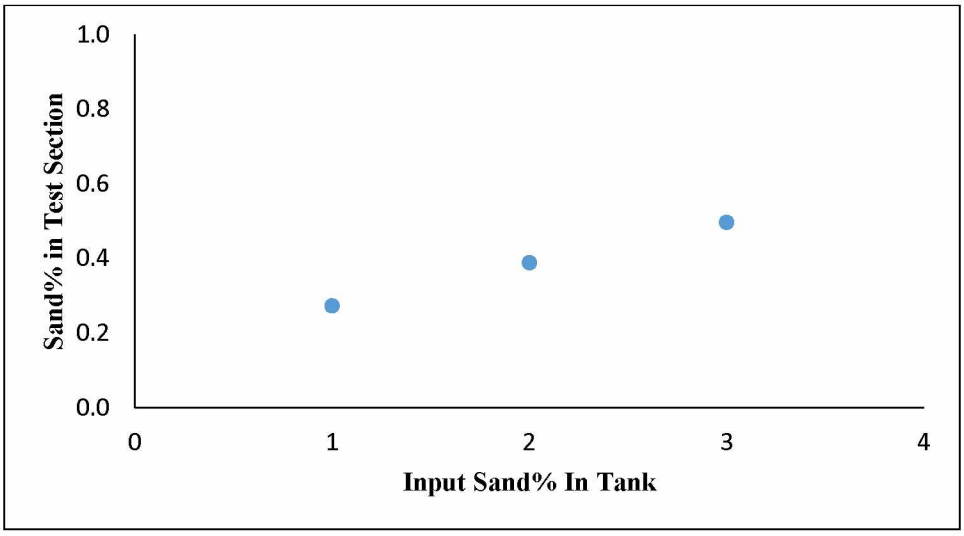

Figure 3.35: Sand Cut in Composite Liquid-Solid-Hold-Up in the Test Section vs Input Sand Concentration for v_{SL} = 0.44/0.45m/s and v_{SG} = 1.66m/s

3.6.4 Three-Phase Oil, Gas and Sand Flow: Differential Pressures

To observe the effects of the presence and varying concentrations of sand in the flow, experiments were performed with similar oil and gas superficial velocities at 1, 2, and 3% sand input concentrations. This was accomplished by using the industrial tank- mounted mixer and adding sand into the oil tank to perform three-phase experiments. Experiments performed from this point on would enable us in understanding the effect of solids in the two-phase oil and gas flow and fulfilling the primary objective of this thesis. Figures 3.36 and 3.37 show effect of the addition of sand on the differential pressure. An increase in pressure drop was observed with tests performed with 1% sand concentration as compared to tests done without sand.

Figures 3.38 and 3.39 show the effect of changing sand concentration in the multiphase flow. There was a minute decrease in differential pressure at v_{SL} = 0.31m/s and an increase at v_{SL} = 0.35m/s with increasing sand concentrations.

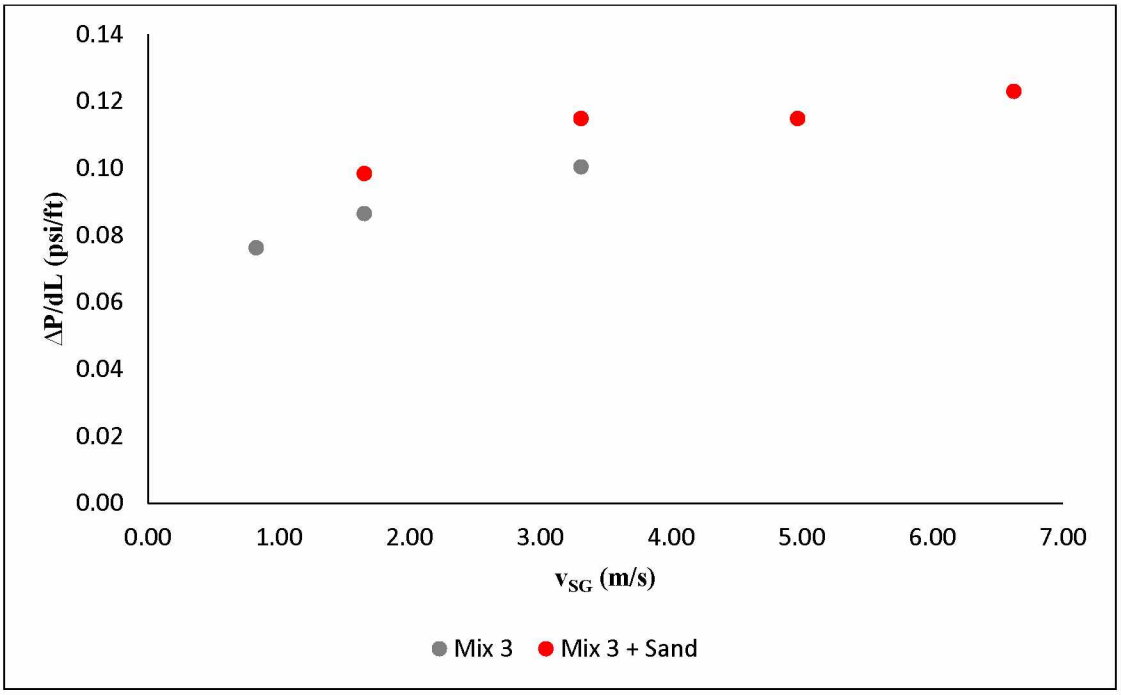

Figure 3.36 Differential Pressure Gradient Comparison, v_{SL} = 0.31m/s

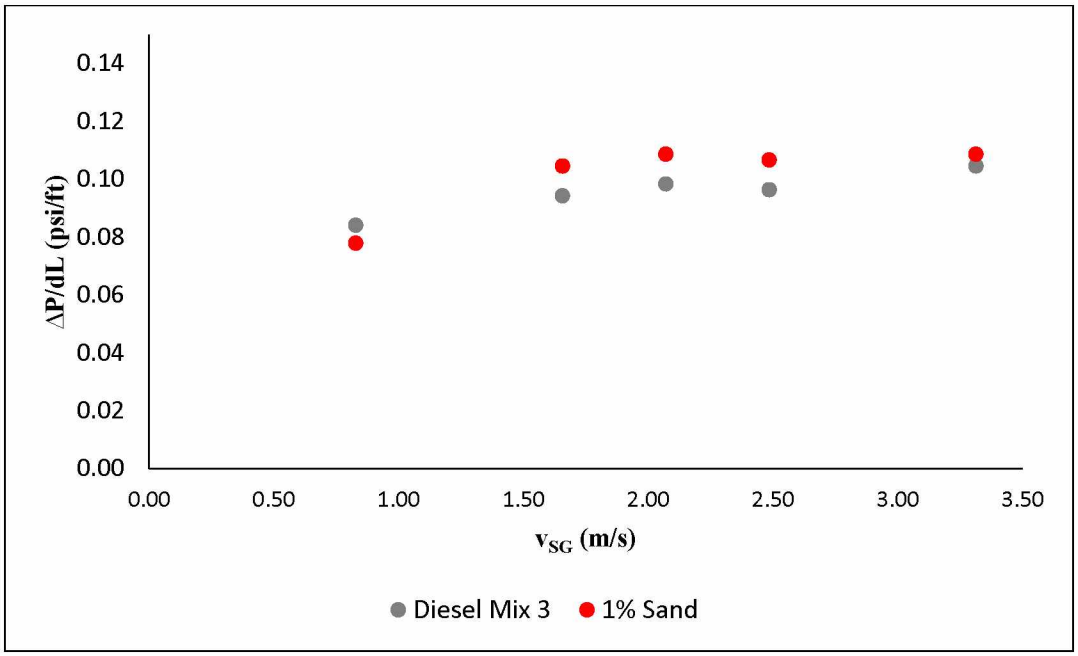

Figure 3.37 Differential Pressure Gradient Comparison, v_{SL} = 0.35m/s

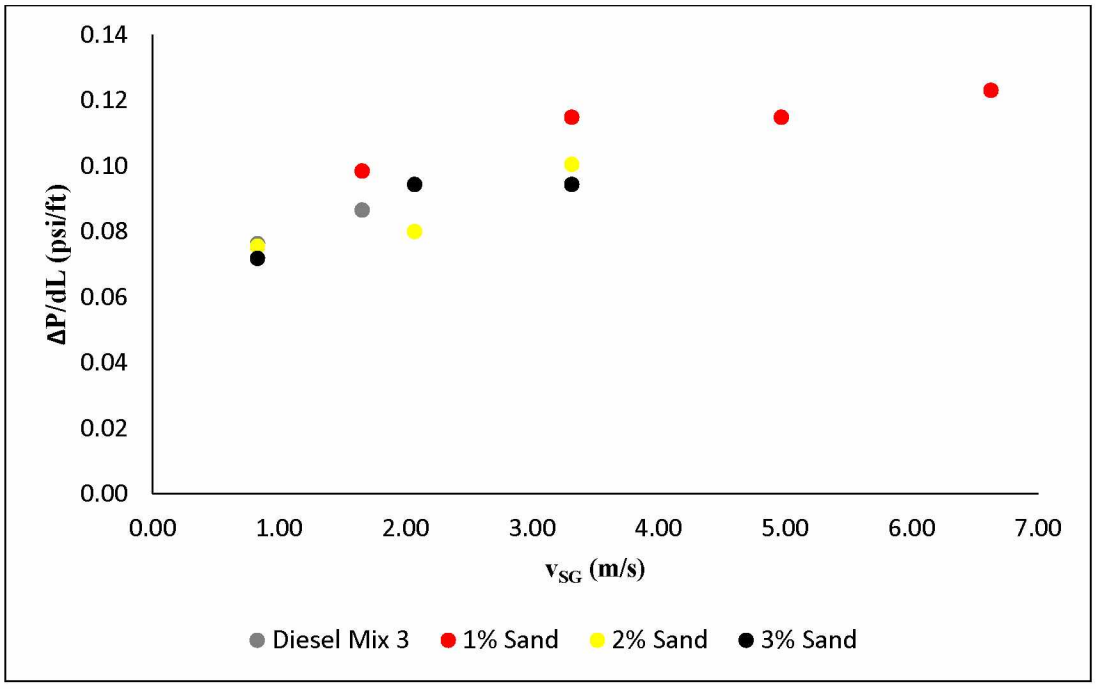

Figure 3.38: Effect of Sand Concentration on Differential Pressure Gradient, v_{SL} = 0.31m/s

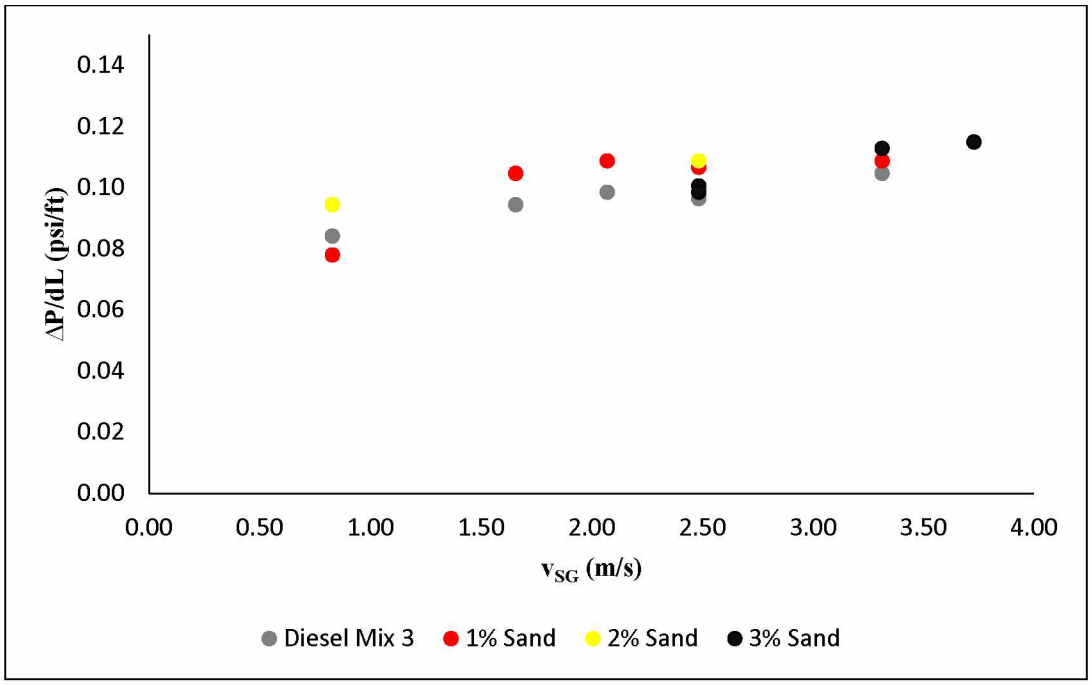

Figure 3.39: Effect of Sand Concentration on Differential Pressure Gradient, v_{SL} = 0.35m/s

The change in differential pressure with changing sand concentrations is not significant enough to be able to confidently comment on the effect of sand concentrations on the flow. This can primarily be attributed to the relatively small changes in sand concentrations in the test section over the range of three-phase flow experiments and secondarily to the intermittent nature of slug flow that lead to data with considerable spread.

3.7 Sources of Errors

The following points highlight the possible sources of errors in the experimental setup

1. Using pump curve to determine oil flow rates hence oil superficial velocities
2. Slippage losses in the pump at low oil flow rates
3. Minimum readable air flow rate on the air flow meter was 2cfm. Air flow rates lower than 2 cfm were approximated from the air flow regulator position.
4. The electrically actuated valves used to trap fluids in the test section for hold-up measurement had a closing time of 10- 12 seconds

5. The liquid and gas phases mixed at a 'T' junction before making three quick 90° turns to enter the test section 10 ft away from these sources of flow disturbances. The bypass line commenced at a 'T' junction at the start of the test section. The test section was about 25ft, shorter than conventional large scale flow loops which may not have provided enough length for flow development. These design restrictions may have accounted for uncertainties related to measuring differential pressure and hold-up.
6. The oil in the tank would become frothy with increasing air rates in two-phase experiments.

Chapter 4

Model Comparisons

4.1 Modeling using PIPESIM

PIPESIM is a steady-state multiphase flow simulator used in the design and analysis of oil and gas wells and pipeline systems.

4.1.1 Differential Pressure Prediction

Data acquired from experiments was utilized in PIPESIM 2013 to predict pressure gradients using the Beggs and Brill Original (1973) and Tulsa Unified Fluid Flow Model (TUFFP Unified) multiphase fluid flow models. A model mimicking the experimental setup was built in PIPESIM and is detailed in Appendix C, experimental input variables were used as input into the software and the results from the two models were compared against experimental data. Figures 4.1 and 4.2 show differential pressure gradient predictions of the two models against 16 experimental data points from the two-phase oil and gas flow and 17 data points for the three-phase oil, gas, and sand flow. This data was used to test model performances for two and three-phase flow. It was realized that the model predictions were within 30% of the observed differential pressure gradients.

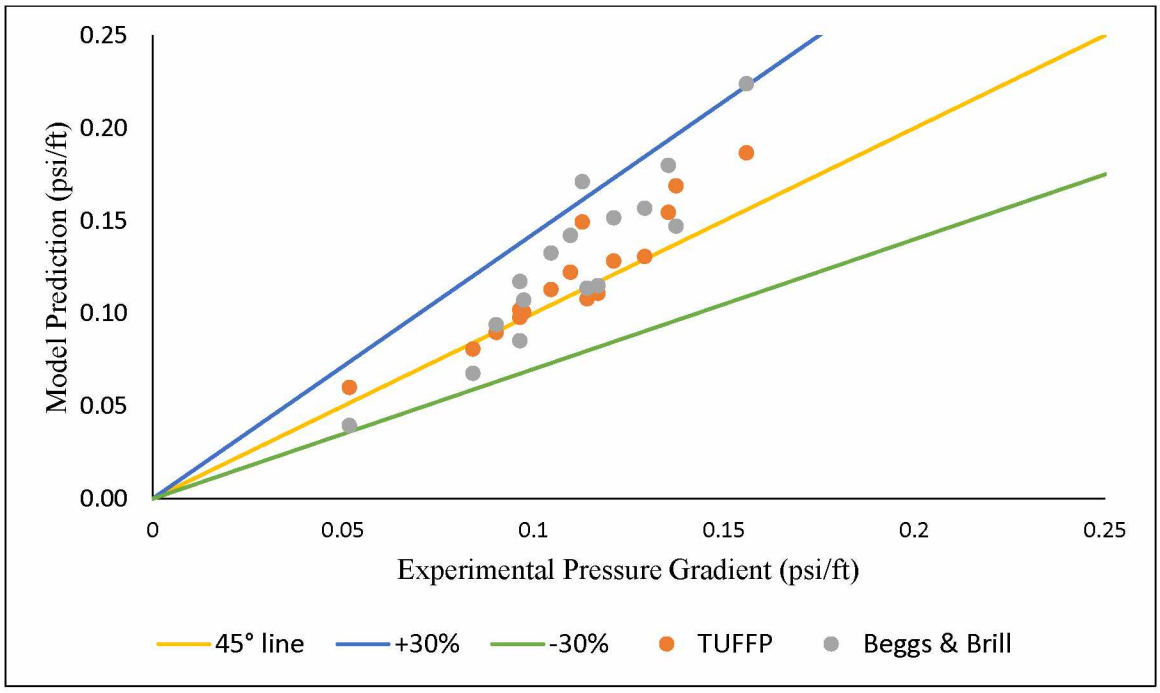

Figure 4.1: ΔP Prediction for Diesel Mix 3 and Gas Data with +/-30% Error Lines

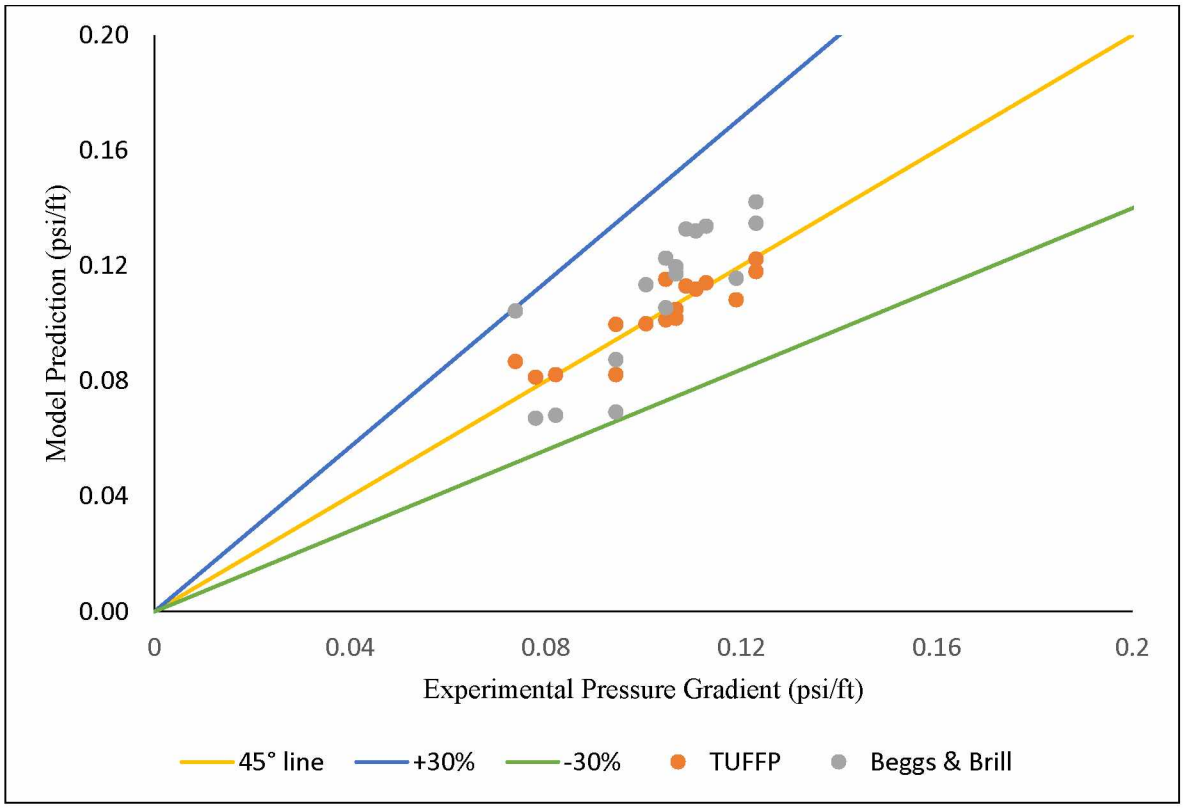

Figure 4.2: ΔP Prediction for Diesel Mix 3, Gas and Sand Data with +/-30% Error Lines

4.1.2 Hold-Up Prediction

Figures 4.3 and 4.4 show the liquid hold-up prediction of the Beggs and Brill Original and TUFFP models for the two-phase oil and gas flow and three-phase oil, gas, and sand flow, respectively. The Beggs and Brill model grossly under-predicted hold-up, falling outside the 30% error range. This model was based on water and air and the results from this study can be contributed to the inapplicability of this model to predict hold-up in viscous oil flow. The TUFFP model on the other hand, which encompasses a large range of fluid viscosities from a growing data bank at the University of Tulsa that is constantly updated, performed satisfactorily.

Overall, the differential pressure predictions from both models were within close range of the observed data for two and three-phase flow. The Beggs and Brill model over-predicted the pressure gradient by an average 6.5% and the TUFFP model over-predicted the pressure gradient by 3.2%.

The TUFFP model was better at predicting liquid hold-ups for both two-phase oil and gas flow as well as the three-phase oil, gas and sand flow. The Beggs and Brill correlation under-predicted liquid hold-up for two-phase flow by an average 83% and 74.5% for three-phase flow; however, the TUFFP model under-predicted hold-up by 5.1 and 0.3% respectively. The TUFFP unified model proved to be more accurate at predicting viscous oil flow behavior than the Beggs and Brill model.

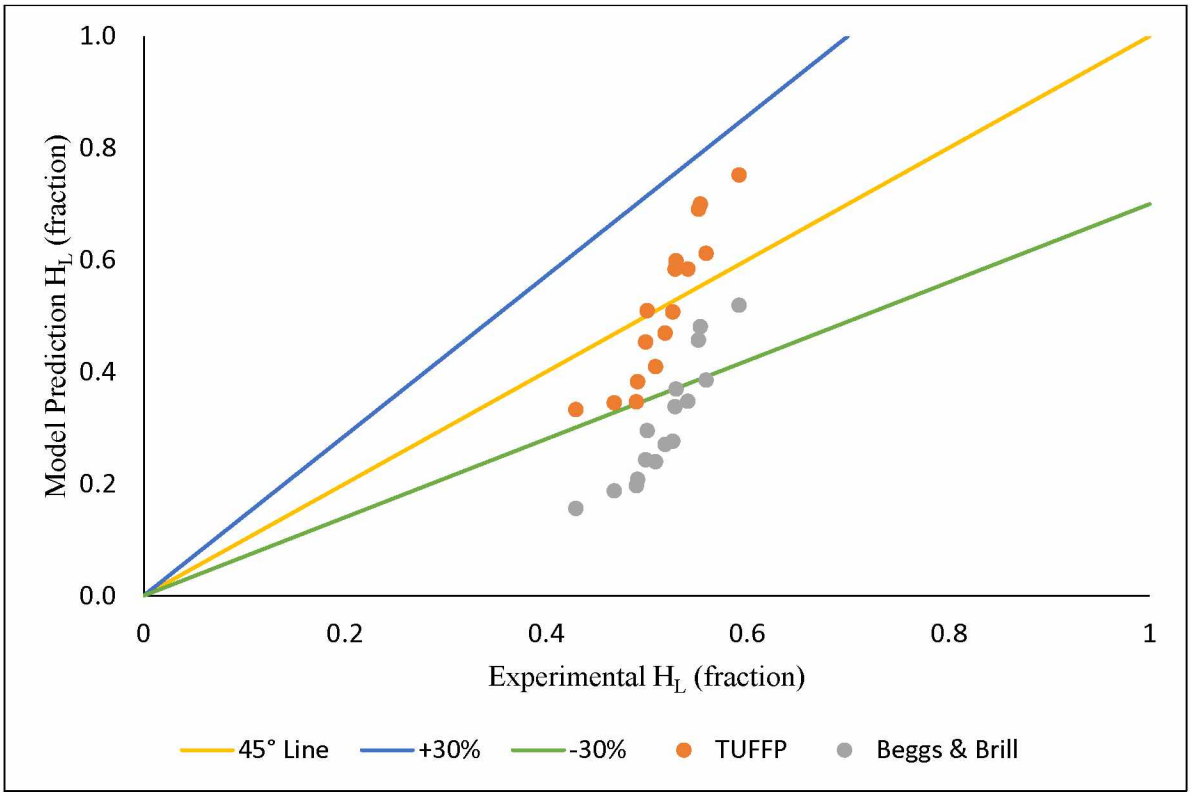

Figure 4.3: Liquid Hold-Up prediction for Diesel Mix 3 and Gas data with +/-30% Error Lines

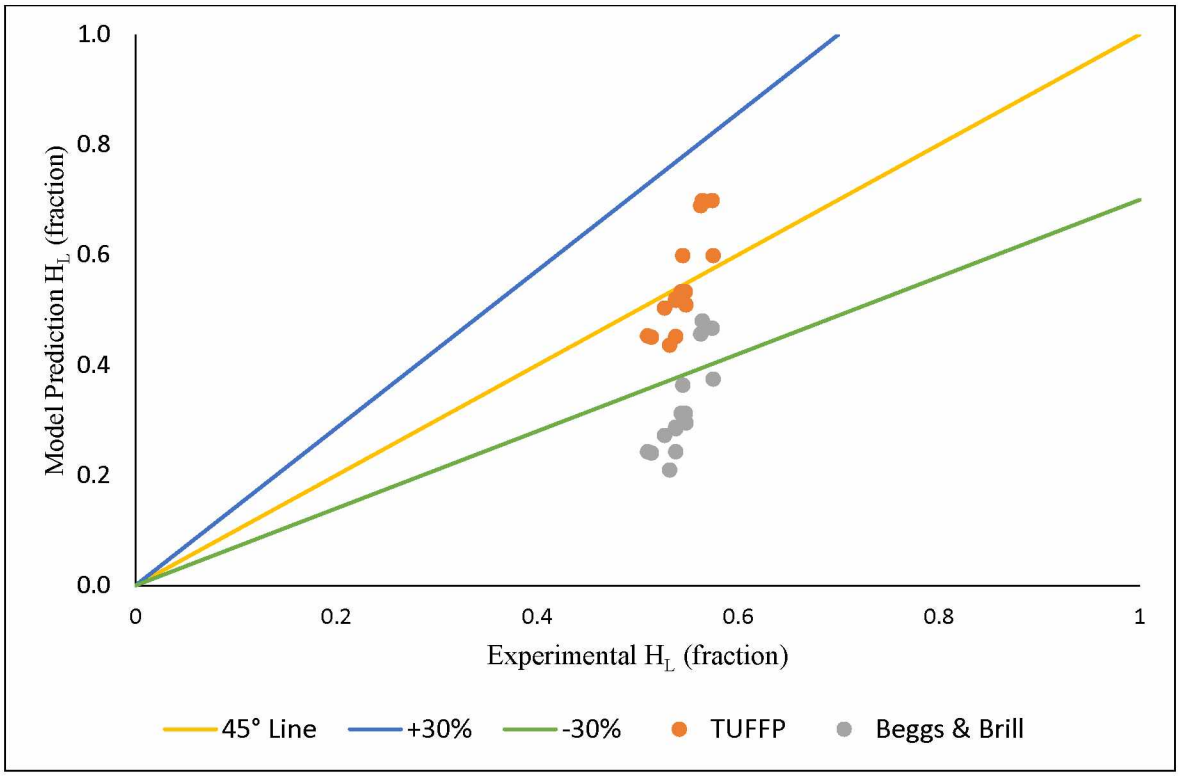

Figure 4.4: Liquid Hold-Up prediction for Diesel Mix 3, Gas and Sand Data (+/-30% Error)

Chapter 5

Slug Flow Analysis and Dimensionless Analysis

5.1 Slug Flow Analysis

Slug flow is the most frequently observed flow pattern in oil and gas wells and pipelines. It was also the most commonly observed flow pattern in this study. It seemed fitting to investigate specific slug flow characteristics in detail from the data gathered from experiments.

5.1.1 Liquid Hold-Up Prediction in Slug Flow

Two models were used to predict liquid hold-up for the slug flow tests performed using the flow loop, Taitel and Barnea (1990) along with a modified version of the Zhao et al. model (2015). The equations from these models focus exclusively on slug flow characteristics. Equations are detailed in Appendix A.

Figures 5.1 through 5.4 show slug unit hold up predictions from the two models against observed values. The data lies within 15% of the predicted hold-up values. This observation may be attributed to a hypothesis that pipe section lengths and the presence or absence "flow development regions" (long sections of undisturbed pipe lengths) may not have an effect on liquid hold-up.

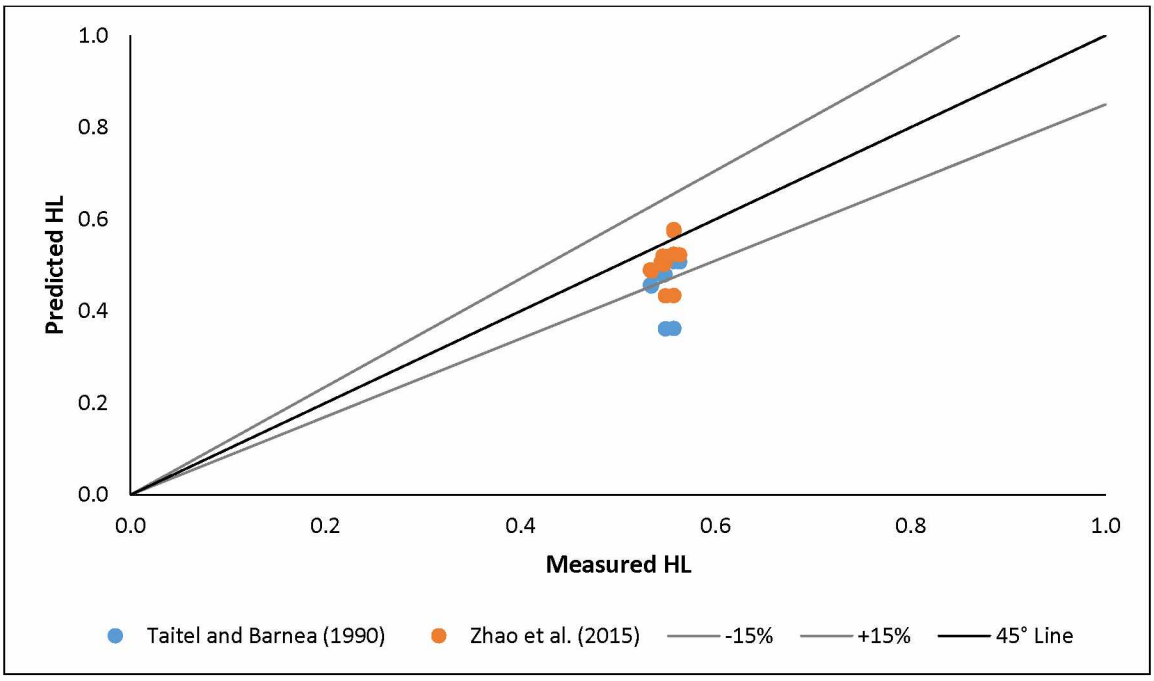

Figure 5.1: Slug Flow Liquid Hold-Up for Diesel Mix 1 with +/- 15% Error Lines

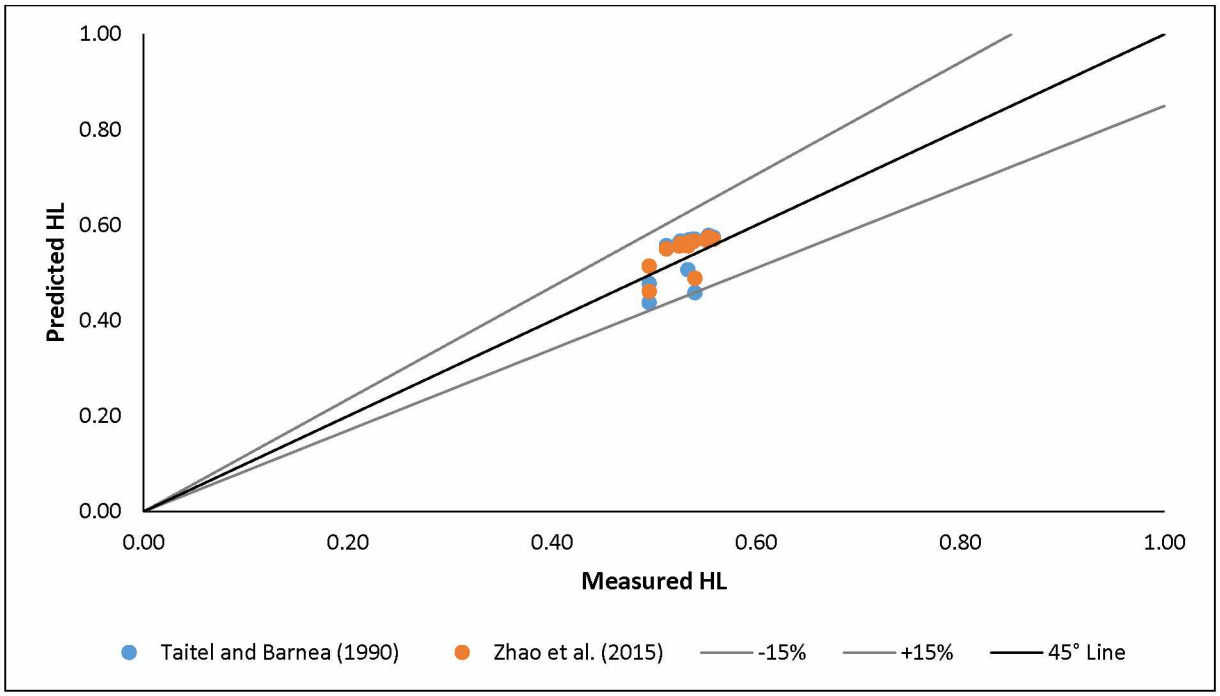

Figure 5.2: Slug Flow Liquid Hold-Up for Diesel Mix 2 with +/- 15% Error Lines

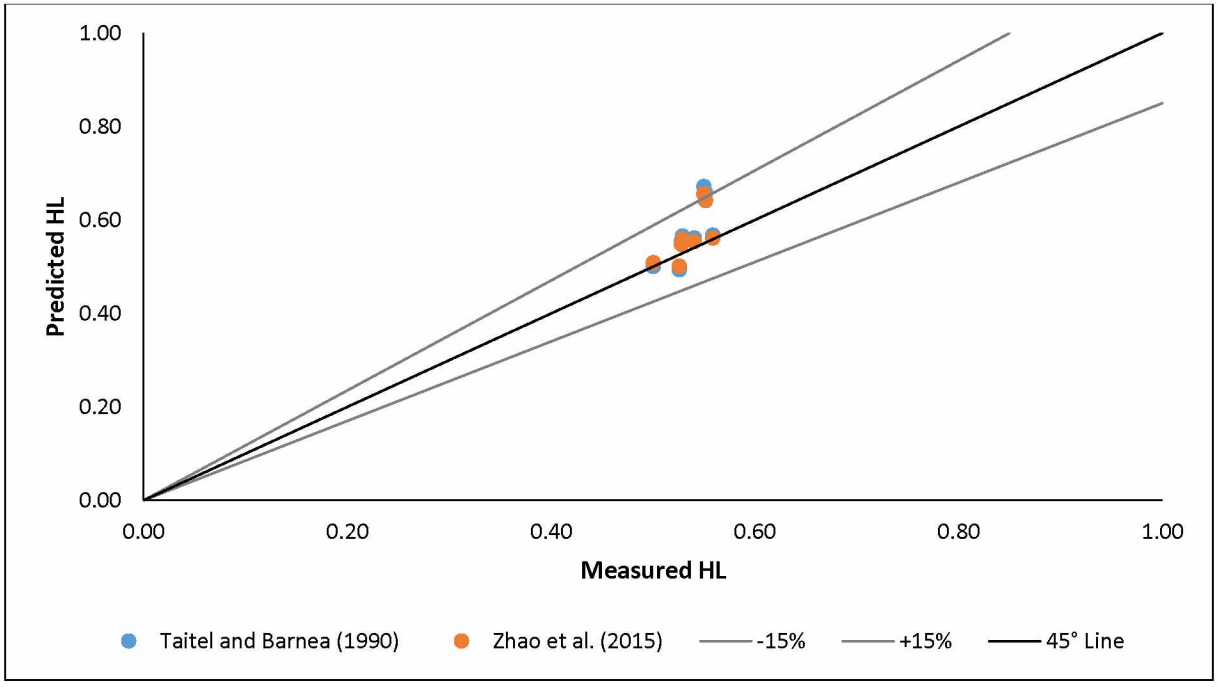

Figure 5.3: Slug Flow Liquid Hold-Up for Diesel Mix 3 with +/- 15% Error Lines

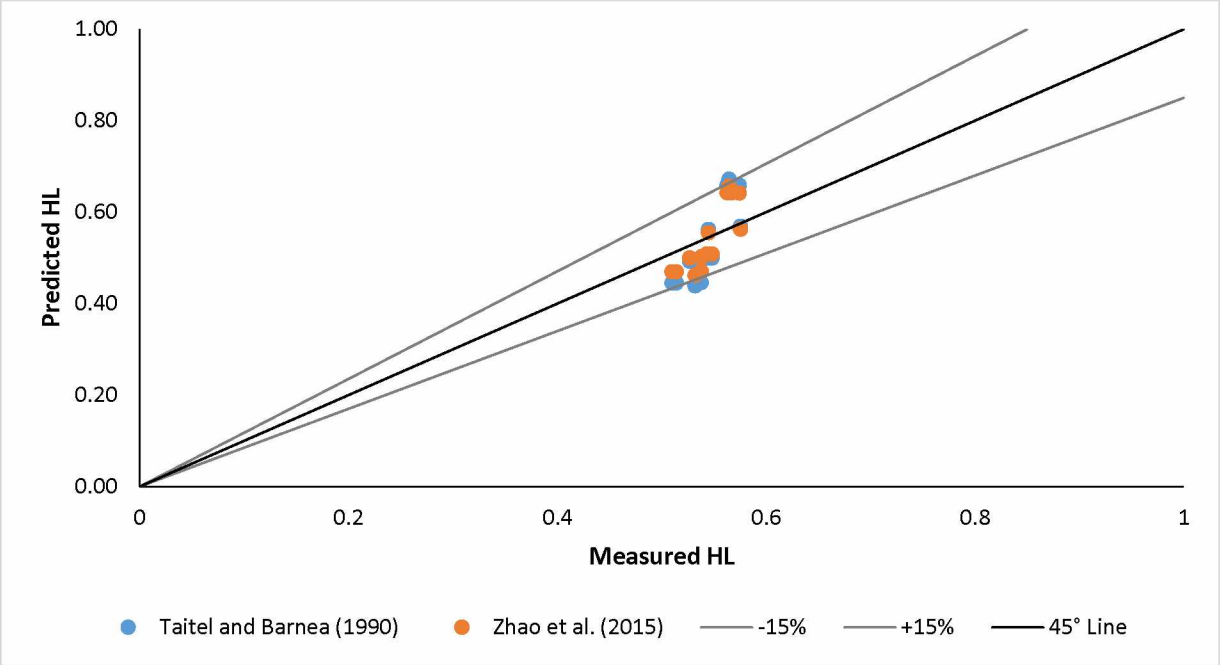

Figure 5.4: Slug Flow Composite Liquid- Solid Hold-Up for Three-Phase Flow (+/- 15% Error)

5.1.2 Slug Length Prediction

Slug Lengths were calculated using the Al-safran et al. (2011) equation for slug length for high viscosity liquid-gas flow:

$$Ls = 2.63D\left(D^{1.5}\sqrt{\rho_L(\rho_L-\rho_G)g}\Big/\mu_L\right)^{0.321} \quad (Eq\ 5.1)$$

Where D is the pipe diameter, ρ_L and ρ_G are liquid and gas densities, g is gravitational acceleration and μ_L is the liquid viscosity, all in S.I units.

Full slug units were filmed using the Casio high speed camera for Diesel Mix 3, sand and gas tests with sand concentrations of 1, 2 and 3% (Figure 5.5). Video enhancements were performed. From nine different oil and gas superficial velocities and sand concentration tests, measurement of slug units revealed an average slug length of 1.39 ft, which was equal to the slug unit length predicted by the Al-safran et al. (2011) correlation.

5.2 Dimensionless Analysis

Chapter 1 outlines the efficacy of using dimensionless groups. It also explains why this approach has been favored in multiphase flow studies to develop correlations. Nine independent variables influencing pressure gradient were identified for the two-phase flow of oil and gas and 11 were identified for the three-phase flow of oil, gas, and sand. Based on these variables, 7 and 9 dimensionless groups were created respectively. Variables, dimensionless groups and correlations are mentioned in Appendix B. For computational simplicity, the 7 dimensionless groups created for the two-phase flow of oil and gas were utilized for analysis of all multiphase flow data.

Figure 5.5: Slug Unit Length Measurement using High Speed Video Camera

Experimental flow parameters for slug flow were used to calculate numerical values of the dimensionless groups for differential pressure analysis and data for all flow patterns was used for hold-up analysis. The calculated numerical values of these groups were normalized and linear regressions were performed in R software. This enabled the identification of the most significant groups responsible for changes in pressure gradient and hold-up, and formulation of equations correlating the dependent and independent groups. Velocity and density ratios, Reynold's Number and the ratio ($\sigma/v_{SL}\ \mu_L$) were determined to be the most influential dimensionless groups on the pressure gradient, highlighted in Appendix B. This result revealed the dependence of differential pressure drop on the input fluid ratio, and liquid properties.

Similarly, regression analysis on liquid hold-up as the dependent variable determined the velocity ratio to be the most significant determining dimensionless group, again highlighting the dependence of liquid hold-up on input fluid ratios and is mentioned in Appendix B. Hold-up data from all flow regimes was used in the regressions to have a higher number of data points.

As stated earlier, Beggs and Brill (1973) had utilized this approach of using dimensionless numbers to perform regression and ascertain the most influential dimensionless groups on liquid hold-up in the two- phase flow of water and air. The dimensionless numbers are defined in Appendix B. Their analysis revealed Froude Number (N_{Fr}) and the input liquid content (λ) to be the most significant parameters on liquid hold-up. As a control test, flow data acquired from the current study was utilized to calculate the numerical values of the dimensionless numbers from Beggs and Brill's study. Normalized linear regression was performed with liquid hold- up considered as the dependent variable. The input liquid content (λ) was determined to be the most significant parameter for the data acquired from this study, similar to the Beggs and Brill study. This test acknowledged the dependence of liquid hold-up on flow parameters such as fluid rates and pipe dimensions rather than fluid characteristics such as fluid composition, viscosity, and density.

Chapter 6

Summary and Conclusions

6.1 Summary

Two and three-phase horizontal flow of heavy oil, gas and sand were experimentally investigated. Experimental data was gathered, analyzed, simulated, and compared with existing correlations and models. Slug flow was investigated in detail.

A unique multiphase flow loop facility was designed and constructed at UAF. A progressive cavity pump was used to flow viscous oil from a double walled steel tank. Compressed air was injected as the gas phase. The facility was sized at 1.5" Schedule 80 PVC plumbing with clear test sections for flow pattern visualization and photography. Equipment issues and operational difficulties in the setup were identified during initial tests and rectified. Oil and gas flow rates, differential and absolute pressures, liquid and composite liquid- solid hold-up, and fluid temperatures were measured and flow pattern observations were photographed and filmed.

Forty-nine single phase and 301 multiphase flow data points were gathered from the facility using oils of 150, 196 and 218 cP viscosities. Flow pattern observations, flow pattern map construction and comparisons were made for two-phase flow of oil and air. Sand was added to the multiphase flow of oil and air in three different concentrations to observe the effects of the presence of solids and their concentration in the flow. Sand cuts were physically measured to identify actual sand concentrations in the flow against added sand in the oil tank. Experimental liquid hold-up and differential pressures were predicted with existing multiphase flow correlations using PIPESIM, a steady-state multiphase flow simulator. Slug flow was studied in detail. Hold-up was predicted using two slug flow models and compared with experimental data. Slug unit length was measured and predicted using a correlation. The dependence of differential pressure gradient and hold-up on independent variables was quantified by identification and creation of dimensionless groups for two and three-phase flows. Normalized linear regression was performed on the dimensionless groups in R using experimental data. The most significant groups were identified for hold-up and differential pressure gradient.

6.2 Conclusions

From the experimental investigation of the two and three-phase flow of heavy oil, gas, and sand, the following observations and conclusions are drawn:

1. A higher pressure drop is observed with increasing oil viscosities in the single phase oil flow and two-phase flow of oil and gas.
2. Six flow patterns are observed in the two-phase flow of oil and gas: Dispersed Bubbly (DB), Elongated Bubbly (EB) Slug (SL), Stratified Wavy (SW), Annular (AN) and Stratified Smooth (SS), all of which occur at distinct oil and gas superficial velocities.
3. The length of elongated bubbles in EB flow increases with increasing gas superficial velocities while the length of slugs in SL flow remains unaffected with changing oil and gas superficial velocities.
4. Based on the flow pattern maps constructed from this study, flow pattern transitions take place at similar oil and gas superficial velocities, indicating independence of these transitions on oil viscosities.
5. A slight increase in differential pressure was noted with increasing oil viscosities. This trend cannot be confirmed because of the minute changes in the magnitude, especially between Diesel Mix 2 and 3, where the viscosity difference between them was only of 20 cP.
6. Liquid hold-up is independent of oil viscosity for the range investigated. It was observed and is thus hypothesized that liquid hold-up is dependent on flow patterns.
7. Addition of sand leads to an increase in pressure drop in the three-phase flow of oil, gas and sand, compared to the two-phase flow of oil and gas. However, increasing concentration of sand did not produce significant changes in pressure drop to affirm a conclusive observation. This can be attributed to the relatively small change in the sand concentration in the test section with the addition of more sand, also to the intermittent nature of slug flow to a certain extent.
8. Increasing sand concentrations in the holding tank linearly manifested themselves as increasing concentrations in the test section.
9. A moving bed of sand can be expected at the bottom of the pipe over the range of oil and gas superficial velocities of 0.25 to 0.41 m/s and 0.5 to 10 m/s respectively

10. Presence of sand in slug flow alters the slug body by distorting eddies on the slug front and the liquid film deposition process at the back. Bubbles in Elongated Bubbly flow lose their sharpness in presence of sand.
11. Flow modelling of two and three-phase flow using the Beggs and Brill and TUFFP models in PIPESIM multiphase flow simulator to predict pressure drop and hold-up produced results within 30 and 15% of the observed data respectively.
12. Liquid hold-up in slug flow using Taitel and Barnea (1990) and Zhao et al. (2015) Slug flow correlations produced results within 15% of the measured hold-up values.
13. Length of a slug unit was accurately predicted by the Al-safran et al. (2011) correlation against measured lengths.
14. Linear regression of dimensionless variables using experimental data suggests that differential pressure gradient and hold-up are significantly dependent on the input liquid and gas ratios groups, the velocity ratio and the input liquid content.

References

Al-safran E., Gokcal, B., & Sarica, C. (2011, June 15). High Viscosity Liquid Effect on Two-Phase Slug Length in Horizontal Pipes. BHR Group.

Aziz, K., & Govier, G. W. (1972, July 1). Pressure Drop In Wells Producing Oil And Gas. Petroleum Society of Canada. doi:10.2118/72-03-04

Beggs, D. H., & Brill, J. P. (1973, May 1). A Study of Two-Phase Flow in Inclined Pipes. Society of Petroleum Engineers. doi:10.2118/4007-PA

Bello, O. O., Udong, I. N., Falcone, G., & Teodoriu, C. (2010, January 1). Hydraulic Analysis of Gas/Oil/Sand Flow in Horizontal Wells. Society of Petroleum Engineers. doi:10.2118/136874-MS

Baxendell, P. B., & Thomas, R. (1961, October 1). The Calculation of Pressure Gradients In High-Rate Flowing Wells. Society of Petroleum Engineers. doi:10.2118/2-PA

Cadrin, D. D. 2015. CHOPS Evolution – Creating CHOPS Contiguously from Toe to Heel in Horizontal Wells, World Heavy Oil Congress 2015, Alberta, Canada

Duns, H., & Ros, N. C. J. (1963, January 1). Vertical flow of gas and liquid mixtures in wells. World Petroleum Congress.

Falcone, G., Teodoriu, C., Reinicke, K. M., & Bello, O. O. (2007, January 1). Multiphase Flow Modelling Based on Experimental Testing: A Comprehensive Overview of Research Facilities Worldwide and the Need for Future Developments. Society of Petroleum Engineers. doi:10.2118/110116-MS

Fancher, G. H., & Brown, K. E. (1963, March 1). Prediction of Pressure Gradients for Multiphase Flow in Tubing. Society of Petroleum Engineers. doi:10.2118/440-PA

Gokcal, B. (2005). Effects of High Oil Viscosity on Two-Phase Oil-Gas Flow Behavior in Horizontal Pipes, Master's Thesis. The University of Tulsa.

Hagedorn, A. R., & Brown, K. E. (1965, April 1). Experimental Study of Pressure Gradients Occurring During Continuous Two-Phase Flow in Small-Diameter Vertical Conduits. Society of Petroleum Engineers. doi:10.2118/940-PA

Han, G., Bruno, M., & Dusseault, M. B. (2007). How Much Oil You Can Get From CHOPS. Petroleum Society of Canada. Canadian International Petroleum Conference, 8-10 June, Calgary,

Alberta. PETSOC-2004-008 http://dx.doi.org/10.2118/2004-008

Hasan, A. R., & Kabir, C. S. (1988, May 1). A Study of Multiphase Flow Behavior in Vertical Wells. Society of Petroleum Engineers. doi:10.2118/15138-PA

May, C. J. (1935, December 1). Efficiency of Flowing Wells. Society of Petroleum Engineers. doi:10.2118/935099-G

Orkiszewski, J. (1967, June 1). Predicting Two-Phase Pressure Drops in Vertical Pipe. Society of Petroleum Engineers. doi:10.2118/1546-PA

Poettman, F. H., & Carpenter, P. G. (1952, January 1). The Multiphase Flow of Gas, Oil, and Water Through Vertical Flow Strings with Application to the Design of Gas-lift Installations. American Petroleum Institute.

Pospisil, G. (2011, January 6). Heavy Oil Challenges and Opportunities North Slope Alaska. Alaska Oil and Gas Association.

Ros, N. C. J. (1961, October 1). Simultaneous Flow of Gas and Liquid As Encountered in Well Tubing. Society of Petroleum Engineers. doi:10.2118/18-PA

Taitel, Y., Barnea, D. (1990) Two Phase Slug Flow. Advances in Heat Transfer, 2, 83-132

Taitel, Y. and Dukler, A. E. (1976), A model for predicting flow regime transitions in horizontal and near horizontal gas-liquid flow. AIChE J., 22: 47–55. doi:10.1002/aic.690220105

Versluys, J. (1930, December 1). Mathematical Development of the Theory of Flowing Oil Wells. Society of Petroleum Engineers. doi:10.2118/930192-G

Zhao, Y., Lao, L., Yeung, H., (2015), Investigation and Prediction of Slug Flow Characteristics in Highly Viscous Liquid and Gas Flows in Horizontal Pipes, Chemical Engineering Research & Design, Volume 102: 124–137

NOMENCLATURE

v_{SL}: Superficial Liquid Velocity, m/s

v_{SG}: Superficial Gas Velocity, m/s

dP/dL: Differential Pressure Gradient, Pa/m and psi/ft

H_L: Liquid Hold-Up and Composite Liquid-Solid Hold-Up

L_S: Slug Unit Length, ft

ρ: Density: Subscript L, G and S: Liquid, Gas and Sand, kg/m^3

μ: Viscosity: Subscript L, G and S: Liquid, Gas and Sand, Pa-s and cP

σ: Surface Tension, N/m and dyne/cm

Appendix A

Single phase oil differential pressure calculations

Using basic fluid flow equations: Darcy- Weisbach equation

$$\Delta P/_L = f_D \rho v^2/_{2D}$$

Where f_D is the Darcy friction factor. All data for single phase fluid flow in this study was laminar, and f_D is a function of Reynolds' Number for laminar flow, given by

$$f_D = 16/_{N_{Re}}$$

Using Bingham Plastic Model equations

$$dP/_{dL} = \mu v/_{1500\, D^2} + \tau_y/_{225\, D}$$

Slug Flow Hold-Up Equations (Zhao et al., 2015)

$$H_{Ls} = 0.85 - 0.0175\varphi + 0.057\sqrt{\varphi^2 + 2.27}$$

$$\varphi = N_{Fr}\, N_{\mu}^{0.2} - 0.89$$

$$N_{Fr} = v_m/_{(gd)^{0.5}} \sqrt{\rho_L/_{(\rho_L - \rho_G)}}$$

$$N_{\mu} = v_m \mu_L/_{(gd)^2(\rho_L - \rho_G)}$$

Appendix B

Dimensionless Groups from Taitel Dukler (1976) Model:

$$X^2 = \frac{\frac{4C_L}{d}\left(\frac{\rho_L v_{SL} d}{\mu_L}\right)^{-n}\frac{\rho_L v_{SL}^2}{2}}{\frac{4C_G}{d}\left(\frac{\rho_G v_{SG} d}{\mu_G}\right)^{-m}\frac{\rho_G v_{SG}^2}{2}}$$

m = n = 1 for laminar flow

$$F = \sqrt{\rho_G/(\rho_L - \rho_G)}\; v_{sG}/\sqrt{dg\cos\theta}$$

$$K^2 = F^2\; \rho_L v_{SL} d/\mu_L$$

Dimensionless Analysis for this study:

Based on content from the course "Multiphase Fluid Flow in Pipes" by Dr. Awoleke at UAF, the following procedure was followed to perform dimensionless analysis:

Step I

Identification of independent variables for Differential Pressure Gradient prediction: The following variables were identified to be influential on the differential pressure gradient for two, and three-phase flow: Nine for two-phase and 10 for three-phase flow, with the differential pressure gradient term being the dependent variable.

Two-Phase oil and gas flow	Three-phase oil, gas and sand flow
a: Superficial liquid velocity (v_{SL})	a: Superficial liquid velocity (v_{SL})
b: Superficial gas velocity (v_{SG})	b: Superficial gas velocity(v_{SG})
c: Oil density (ρ_L)	c: Superficial sand velocity (v_{SS})
d: Gas density (ρ_G) (ρ_G)	d: Oil density (ρ_L)
e: Oil viscosity (μ_L) (μ_L)	e: Gas density(ρ_G)

f: Gas viscosity (μ_G)	f: Sand density (ρ_S)
g: Oil- gas surface tension (σ)	g: Oil viscosity (μ_L)
h: Pipe diameter (D)	h: Gas viscosity(μ_G)
i: Gravitational acceleration (g)	i: Oil- gas surface tension (σ)
-	j: Gravitational acceleration (g)

Note: The following steps highlight the procedure for the two-phase dimensionless analysis

Step II

The units of all variables were identified and grouped into three equations based on the fundamental quantities of Mass, Length and Time [MLT] components. For example, superficial gas velocity (a : v_{SL}) would have the fundamental units $[M^0L^1T^{-1}]^a$

Step III

Once these variables were defined into their [MLT] components, the individual M, L and T components of each variable were grouped together to form the following 3 equations. In those 3 equations, we have 10 unknowns: Nine variables defined in Step I and the differential pressure gradient being the tenth.

$$M = c + d + e + f + g + j$$

$$L = a + b - 3c - 3d - e - f + h + i - 2j$$

$$T = -a - b - e - f - 2g - 2i - 2j$$

Step IV

The equations were used in their matrix forms and converted to row echelon matrices. The rank of the resulting matrix was 7, meaning we can expect 7 dimensionless groups. Converting the matrix back to equations, we get:

$$a + b + g - h + 3i + 3j = 0$$

$$c + d - h + i + 2j = 0$$

$$e + f + g + h - i - j = 0$$

Step V:

Formulate the first dimensionless group π_1, by assuming $b = 1$, giving $a = -1, and\ the\ rest\ of\ the\ variables = 0$. Hence the first dimensionless group would be $\pi_1 = {v_{SG}}/{v_{SL}}$

Similarly, set c though j = 1 to get the rest of the 6 dimensionless groups:

Dimensionless Groups

$$\pi_1 = {v_{SG}}/{v_{SL}}$$

$$\pi_2 = {\rho_G}/{\rho_L}$$

$$\pi_3 = {\mu_G}/{\mu_L}$$

$$\pi_4 = {\sigma}/{v_{SL}\,\mu_L}$$

$$\pi_5 = {v_{SL}D\rho_L}/{\mu_L}$$

$$\pi_6 = {g\mu_L}/{\rho_L v_{SL}}$$

$$\pi_7 = \left(\frac{dP}{dL}\right)\mu_L \Big/ \rho_L v_{SL}^2$$

Following the same the procedure to obtain dimensionless groups for the three-phase flow of oil, gas and sand:

$$\pi'_1 = {v_{SG}}/{vs_L}$$

$$\pi'_2 = {v_{SS}}/{vs_L}$$

$$\pi'_3 = {\rho_G}/{\rho_L}$$

$$\pi'_4 = {\rho_S}/{\rho_L}$$

$$\pi'_5 = {\mu_G}/{\mu_L}$$

$$\pi'_6 = {\sigma}/{v_{S_L}\,\mu_L}$$

$$\pi'_7 = {v_{SL}\mathrm{D}\rho_L}/{\mu_L}$$

$$\pi'_8 = {g\mu_L}/{\rho_L v_{SL}^3}$$

$$\pi'_9 = \left(\frac{dP}{dL}\right)\mu_L \Big/ \rho_L{}^2 v_{SL}^3$$

Linear Regression Result with π_7 dependent variable

```
Call:
lm(formula = Pi7 ~ Pi1 + Pi2 + Pi3 + Pi4 + Pi5 + Pi6, data = regress_data)

Residuals:
      Min        1Q    Median        3Q       Max
-0.170934 -0.015603  0.001053  0.015987  0.192295

Coefficients: (1 not defined because of singularities)
            Estimate Std. Error t value Pr(>|t|)
(Intercept) -0.01639    0.02183  -0.751 0.455576
Pi1          0.10437    0.02568   4.064 0.000142 ***
Pi2         -0.07079    0.01438  -4.923 7.00e-06 ***
Pi3               NA         NA      NA       NA
Pi4          1.27370    0.28649   4.446 3.84e-05 ***
Pi5          0.26181    0.02791   9.382 2.26e-13 ***
Pi6         -0.22137    0.29545  -0.749 0.456610
---
Signif. codes:  0 '***' 0.001 '**' 0.01 '*' 0.05 '.' 0.1 ' ' 1

Residual standard error: 0.04036 on 60 degrees of freedom
Multiple R-squared:  0.9837,    Adjusted R-squared:  0.9823
F-statistic: 722.5 on 5 and 60 DF,  p-value: < 2.2e-16
```

$$\pi_7 = 0.104\pi_1 - 0.071\pi_2 + 1.27\pi_4 + 0.262\pi_5 - 0.221\pi_6$$

Normalized Linear Regression Results

The significance of above equation is that the value of π_7, that houses the differential pressure gradient term, can be calculated by using experimental data of the independent variable. This equation was developed using slug flow data from the two and three-phase flow experiments. 66 data points were used to develop the equation with an adjusted R-squared value of 0.9861.

Independent variables for Liquid Hold-Up

a: Superficial liquid velocity (v_{SL})
b: Superficial gas velocity (v_{SG})
c: Oil density (ρ_L)
d: Gas density (ρ_G) (ρ_G)
e: Oil viscosity (μ_L) (μ_L)
f: Gas viscosity (μ_G)
g: Oil- gas surface tension (σ)
h: Pipe diameter (D)
i: Gravitational acceleration (g)

Dimensionless Groups:

$$\pi_1 = {}^{vsg}/_{vs_L}$$

$$\pi_2 = {}^{\rho_G}/_{\rho_L}$$

$$\pi_3 = {}^{\mu_G}/_{\mu_L}$$

$$\pi_4 = {}^{\sigma}/_{vs_L\,\mu_L}$$

$$\pi_5 = {}^{v_{SL}D\rho_L}/_{\mu_L}$$

$$\pi_6 = {}^{g\mu_L}/_{\rho_L v_{SL}^3}$$

Normalized Linear Regression Results with $\pi_7 = H_L$ dependent variable:

```
Coefficients: (1 not defined because of singularities)
            Estimate Std. Error t value Pr(>|t|)
(Intercept)  -0.2732     0.2806  -0.974 0.336889
Pi1          -0.4974     0.1305  -3.811 0.000538 ***
Pi2          -0.1248     0.1848  -0.676 0.503776
Pi3              NA         NA      NA       NA
Pi4           2.8829     2.8113   1.025 0.312187
Pi5           0.9329     0.8691   1.073 0.290439
Pi6          -1.7661     2.0301  -0.870 0.390261
---
Signif. codes:  0 '***' 0.001 '**' 0.01 '*' 0.05 '.' 0.1 ' ' 1

Residual standard error: 0.3016 on 35 degrees of freedom
Multiple R-squared:  0.5197,    Adjusted R-squared:  0.4511
F-statistic: 7.574 on 5 and 35 DF,  p-value: 6.581e-05
```

$$\pi_7 = -0.497\pi_1 - 0.125\pi_2 + 2.88\pi_4 + 0.933\pi_5 - 1.77\pi_6$$

Normalized Linear Regression Results

Similar to linear regression performed to correlate the differential pressure gradient with the independent variables, the hold-up is correlated to the independent variables yielding the following equation. The low adjusted R-squared value of 0.45 is a result of the inclusion of hold-up data of all flow regimes as opposed to only slug flow data. This was done in order to have a large number of data points (42) to develop the correlation.

Dimensionless Groups used by Beggs and Brill (1973)
Liquid Velocity Number N_{LV}
Gas Velocity Number: N_{GV}
Pipe Diameter Number: N_D

Reynolds' Number: N_{Re}
Froude Number: N_{Fr}
Pressure ratio: $^{p}/_{p_a}$
Gas Liquid Ratio: $^{q_g}/_{q_L}$
Input liquid content: λ

Appendix C

PIPESIM Model specifications

Parameter	Value
Pipe Length	24.375ft, Horizontal
Pipe Diameter	1.5"
Viscosity Model	User defined, two-point
Test Temperature	67.8°F
Water Cut	0

Liquid flowrate, gas flowrate, GOR and Inlet Pressure data was used from experiments in the simulations.

Experimental Data

Diesel Mix 1			
v_{SL} (m/s)	v_{SG} (m/s)	$(^{d_P}/_{d_L})$ (psi/ft)	$(^{d_P}/_{d_L})$ (Pa/m)
0.07	0.21	0.008	190
0.07	0.41	0.010	237
0.07	1.04	0.012	278
0.07	2.07	0.015	329
0.07	3.52	0.033	742
0.07	4.56	0.025	557
0.07	5.18	0.023	510
0.07	6.21	0.017	385
0.07	7.87	0.021	483
0.07	9.11	0.027	622
0.07	10.35	0.034	770
0.09	0.21	0.011	255
0.09	0.31	0.014	325

0.09	0.83	0.014	320
0.09	2.07	0.016	367
0.09	2.90	0.022	501
0.09	4.14	0.015	343
0.08	4.97	0.030	687
0.08	5.80	0.019	427
0.08	6.63	0.022	487
0.08	7.45	0.025	557
0.08	8.28	0.027	603
0.08	9.32	0.032	724
0.11	0.21	0.015	331
0.11	0.83	0.018	399
0.11	3.31	0.023	510
0.11	5.38	0.025	557
0.10	9.94	0.042	940
0.18	0.21	0.022	496
0.18	1.24	0.030	676
0.18	2.90	0.033	750
0.18	3.73	0.041	920
0.18	5.38	0.049	1105
0.17	6.83	0.052	1173
0.17	7.66	0.051	1146
0.17	9.94	0.057	1297
0.27	0.21	0.033	747
0.27	0.41	0.035	785
0.27	1.45	0.043	970
0.27	2.89	0.055	1253
0.26	3.51	0.059	1346
0.26	4.13	0.068	1531
0.26	4.55	0.064	1438
0.26	4.96	0.074	1670
0.26	5.79	0.084	1902
0.26	7.85	0.090	2042
0.57	0.21	0.071	1597
0.57	0.31	0.071	1608
0.57	0.41	0.073	1650
0.57	1.04	0.137	3092
0.57	2.48	0.087	1974
0.54	3.52	0.078	1767
0.54	4.97	0.118	2675
0.64	0.10	0.079	1777

0.64	0.21	0.079	1783
0.64	0.31	0.080	1801
0.64	0.41	0.087	1969
0.64	2.07	0.094	2116
0.64	3.31	0.116	2622
0.74	0.06	0.090	2043
0.74	0.10	0.096	2167
0.74	0.21	0.100	2252
0.74	0.41	0.105	2386
0.74	1.66	0.117	2638
0.73	3.11	0.134	3020
0.34	8.90	0.123	2784
0.35	8.90	0.127	2877
0.52	8.90	0.185	4176

v_{SL} (m/s)	v_{SG} (m/s)	Flow Regime	$(^{d_P}/_{d_L})$ (psi/ft)	$(^{d_P}/_{d_L})$ (Pa/m)	H_L
0.04	3.73	SW	0.007	167	0.46
0.04	3.73	SW	0.009	213	0.46
0.06	4.56	SW	0.012	278	0.44
0.06	4.56	SW	0.012	269	0.44
0.49	2.90	SL	0.107	2413	0.54
0.49	3.31	SL	0.113	2552	0.53
0.50	2.48	SL	0.094	2134	0.56
0.51	1.66	SL/EB	0.092	2088	0.56
0.51	0.72	EB	0.070	1578	0.63
0.49	0.52	EB	0.073	1652	0.63
0.49	1.66	SL	0.086	1949	0.56
0.49	2.48	SL	0.107	2413	0.56
0.49	2.90	SL	0.113	2552	0.55
0.46	0.62	EB	0.069	1559	0.69
0.46	1.66	SL	0.086	1949	0.56
0.45	0.66	EB	0.066	1485	0.67
0.45	1.66	SL	0.074	1670	0.55
0.43	0.62	EB	0.063	1429	0.67
0.41	0.66	EB	0.057	1299	0.65
0.40	0.66	EB	0.053	1206	0.67
0.46	2.48	SL	0.098	2227	0.55
0.46	2.90	SL	0.103	2320	0.55
0.47	3.31	SL	0.115	2598	0.53
0.45	2.48	SL	0.086	1949	0.55

0.24	8.70	AN	0.074	1670	0.40
0.26	7.45	AN	0.096	2181	0.43
0.28	5.38	SW/AN	0.078	1763	0.45
0.66	0.04	DB	0.086	1949	0.89
0.68	0.04	DB	0.092	2088	0.83
0.70	0.04	DB	0.094	2134	0.78
0.71	0.04	DB	0.094	2134	0.90
0.35	9.73	AN	0.139	3155	

Diesel Mix 2				
v_{SL} (m/s)	v_{SG} (m/s)	Flow Regime	$(^{d_P}/_{d_L})$(psi/ft)	$(^{d_P}/_{d_L})$(Pa/m)
0.31	0.83	EB	0.073	1652
0.31	1.66	SL	0.084	1902
0.30	3.31	SL	0.105	2366
0.30	5.38	SL/SW	0.117	2645
0.30	6.63	SW	0.113	2552
0.30	8.28	SW	0.119	2691
0.30	9.53	SW	0.128	2886
0.21	0.41	EB	0.044	993
0.20	1.24	EB/SL	0.051	1146
0.20	1.66	SL	0.055	1234
0.20	2.90	SL	0.062	1392
0.20	3.73	SL/SW	0.071	1596
0.20	5.80	SW	0.069	1559
0.20	7.87	SW	0.086	1949
0.41	0.33	EB	0.077	1735
0.41	1.04	EB/SL	0.090	2042
0.40	3.31	SL	0.123	2784
0.40	7.04	AN	0.150	3387
0.41	4.14	SL/AN	0.139	3155
0.41	4.97	AN	0.142	3202
0.42	1.66	SL	0.098	2227
0.43	1.66	SL	0.111	2506
0.44	1.66	SL	0.117	2645
0.45	1.66	SL	0.119	2691
0.47	1.66	SL	0.115	2598
0.47	2.48	SL	0.131	2970
0.49	2.07	SL	0.123	2784
0.49	4.97	SW?	0.162	3666
0.48	9.94	AN	0.195	4408
0.08	1.24	SL	0.019	436
0.08	2.07	SL	0.025	557
0.08	3.73	SL/SW	0.023	520
0.08	4.97	SW	0.025	557
0.08	6.21	SW	0.030	687
0.07	8.28	SW	0.040	908
0.26	3.73	SL/SW	0.080	1810
0.26	4.97	SL/SW?	0.082	1856
0.26	5.80	SW	0.101	2274
0.26	6.63	SW	0.101	2274
0.26	7.87	SW	0.096	2181
0.49	1.24	SL	0.103	2320
0.49	2.07	SL	0.112	2543

0.49	2.90	SL	0.133	3016
0.49	3.73	SL	0.174	3944
0.49	4.97	SL/AN	0.185	4176
0.49	6.21	AN	0.185	4176
0.49	7.66	AN	0.180	4074

v_{SL} (m/s)	v_{SG} (m/s)	Flow Regime	$(^{dP}/_{dL})$ (psi/ft)	$(^{dP}/_{dL})$ (Pa/m)	H_L
0.53	0.50	EB	0.100	2264	0.65
0.53	1.66	SL	0.113	2552	0.55
0.52	3.31	SL	0.144	3248	0.54
0.49	1.66	SL	0.107	2413	0.56
0.48	1.66	SL	0.103	2320	0.55
0.46	1.66	SL	0.098	2227	0.54
0.45	1.66	SL	0.096	2181	0.53
0.43	1.66	SL	0.090	2042	0.53
0.40	1.66	SL	0.084	1902	0.52
0.36	1.66	SL	0.078	1763	0.51
0.26	5.38	AN/SW	0.092	2088	0.46
0.29	5.38	AN/SW	0.113	2552	0.47
0.30	6.83	SW	0.127	2877	0.41
0.08	0.31	EB	0.019	436	0.92
0.08	0.10	SS	0.021	464	0.53
0.25	0.83	EB	0.062	1392	0.56
0.25	3.31	SL	0.078	1763	0.50
0.25	4.56	SL/SW	0.096	2181	0.47
0.24	7.45	?	0.102	2302	0.42
0.24	9.11	?	0.119	2682	0.40
0.43	8.28	AN/SW	0.144	3248	0.44
0.44	3.31	SL	0.139	3155	0.53
0.46	0.04	DB/EB/SL	0.090	2042	0.76
0.46	0.04	DB	0.089	2005	0.89
0.43	9.11		0.181	4083	0.45

Diesel Mix 3				
v_{SL} (m/s)	v_{SG} (m/s)	Flow Regime	$(^{dP}/_{dL})$ (psi/ft)	$(^{dP}/_{dL})$ (Pa/m)
0.21	1.24	SL	0.057	1281
0.21	1.66	SL	0.061	1373

0.20	2.90	SL/SW	0.061	1383
0.20	3.73	SL/SW	0.070	1578
0.20	5.80	SW	0.074	1670
0.20	8.28	SW	0.091	2069
0.31	0.83	EB	0.076	1726
0.31	1.66	SL	0.087	1958
0.31	3.31	SL	0.101	2274
0.30	4.97	SL/SW	0.109	2459
0.30	6.63	SW	0.113	2552
0.30	8.28	SW	0.119	2691
0.30	9.53	SW/AN	0.138	3127
0.26	0.83	SL	0.070	1578
0.25	1.24	SL	0.071	1615
0.25	3.31	SL	0.086	1949
0.25	4.56	SW	0.087	1967
0.24	7.45	SW	0.103	2320
0.24	9.11	SW/AN	0.119	2691
0.35	1.66	SL	0.094	2134
0.35	2.07	SL	0.098	2227
0.35	2.69	SL	0.109	2459
0.34	3.31	SL-SW	0.109	2459
0.38	1.86	SL	0.107	2413
0.38	2.48	SL	0.117	2645
0.38	3.52	SL/SW	0.123	2784
0.42	1.66	SL	0.119	2691
0.42	2.48	SL	0.129	2923
0.41	3.73	SL/SW	0.137	3109
0.45	3.93	SL/SW	0.152	3434
0.45	1.86	SL	0.121	2738
0.46	1.24	EB/SL	0.113	2552

v_{SL} (m/s)	v_{SG} (m/s)	Flow Regime	$(^{d_P}/_{d_L})$ (psi/ft)	$(^{d_P}/_{d_L})$ (Pa/m)	H_L
0.44	1.66	SL	0.117	2645	0.56
0.42	1.66	SL	0.114	2580	0.53
0.39	1.66	SL	0.097	2204	0.54
0.35	1.66	SL	0.090	2042	0.53
0.35	0.83	EB/SL	0.084	1902	0.55
0.42	0.83	EB-SL	0.096	2181	0.55
0.41	2.48	SL	0.110	2482	0.50
0.41	3.31	SL/SW	0.129	2923	0.52
0.41	4.14	SL/SW	0.135	3062	0.51
0.41	5.80	SW	0.156	3526	0.49
0.35	3.31	SL/SW	0.105	2366	0.50
0.35	2.48	SL	0.096	2181	0.53
0.34	4.56	SL/SW	0.121	2738	0.49
0.34	5.80	SW	0.113	2552	0.47
0.34	8.28	SW	0.137	3109	0.43
0.27	0.41	EB	0.052	1169	0.59
0.27	1.24	EB/SL	0.059	1327	

Diesel Mix 3 + Sand				
v_{SL} (m/s)	v_{SG} (m/s)	Flow Regime	$(^{d_P}/_{d_L})$ (psi/ft)	$(^{d_P}/_{d_L})$ (Pa/m)
1% Sand				
0.45	1.24	EB/SL	0.117	2645
0.46	0.41	EB	0.100	2264
0.45	1.86	SL	0.125	2830
0.45	2.48	SL	0.135	3062
0.45	3.31	SL	0.137	3109
0.45	0.41	SL/SW	0.153	3452
0.44	6.63	SW	0.187	4223
0.44	7.45	SW	0.178	4037
0.44	9.11	AN	0.168	3805
0.44	10.35	AN	0.178	4037
0.45	5.80	SW	0.146	3294
0.30	0.83	SL	0.088	1986

0.31	1.66	SL	0.098	2227
0.31	3.31	SL/SW	0.115	2598
0.31	4.97	SW	0.115	2598
0.31	6.63	SW	0.123	2784
0.30	8.28	SW/AN	0.135	3062
0.30	9.53	AN/SW	0.150	3387
0.35	1.66	SL	0.105	2366
0.35	2.07	SL	0.109	2459
0.34	3.31	SL/SW	0.121	2738
0.34	4.56	SW	0.131	2970
0.34	6.63	SW/AN	0.135	3062
0.34	7.45	AN	0.133	3016
0.33	9.32	AN	0.154	3480
0.25	1.24	SL/EB	0.069	1559
0.25	3.31	SL	0.078	1763
0.25	5.38	SW	0.090	2042
0.41	1.66	SL	0.121	2738
0.41	4.14	SL/AN	0.148	3341
0.41	5.80	AN	0.156	3526
0.42	3.31	SL	0.135	3062
0.38	6.21	SW	0.133	3016
0.38	4.97	SW	0.139	3155
0.39	1.66	SL	0.101	2274
0.39	0.83	EB/SL	0.096	2181
0.38	3.52	SL/SW	0.129	2923
0.27	6.83	SW	0.096	2181
0.28	4.35	SW	0.103	2320
0.28	2.48	SL	0.072	1624
0.28	1.24	EB/SL	0.070	1578
0.28	0.83	EB	0.066	1485
0.20	8.28	SW	0.077	1745
0.20	5.80	SW	0.064	1438
0.20	3.73	SL/SW	0.066	1485
0.20	2.90	SL	0.057	1299
0.20	1.66	SL	0.055	1253
0.21	0.50	EB	0.039	882
2% Sand				
0.42	1.66	SL/EB	0.119	2691
0.25	3.31	SL	0.078	1763
0.26	1.24	EB-SL	0.070	1578
0.25	5.38	SL/SW	0.109	2459

0.26	4.14	SL	0.092	2088
0.31	0.83	EB/SL	0.075	1708
0.30	8.28	SW	0.121	2738
0.31	2.07	SL	0.080	1810
0.31	3.31	SL	0.101	2274
0.35	2.48	SL	0.109	2459
0.34	3.73	SL	0.111	2506
0.34	4.97	SL/SW	0.123	2784
3% Sand				
0.35	2.48	SL	0.098	2227
0.35	3.73	SL	0.115	2598
0.34	4.97	SL/SW	0.129	2914
0.31	0.83	EL/SL	0.072	1624
0.31	2.07	SL	0.094	2134
0.31	3.31	SL	0.094	2134
0.26	0.83	EB/SL	0.064	1438
0.25	2.07	SL	0.080	1810
0.25	1.66	SL	0.064	1438
0.26	1.24	SL/EB	0.062	1392

v_{SL} (m/s)	v_{SG} (m/s)	Flow Regime	$(^{d_P}/_{d_L})$ (psi/ft)	$(^{d_P}/_{d_L})$ (Pa/m)	H_L
1% Sand					
0.27	3.31	SL	0.074	1670	0.53
0.35	0.83	EB/SL	0.078	1763	0.57
0.35	3.31	SL	0.109	2459	0.51
0.41	2.48	SL	0.123	2784	0.55
0.40	1.66	SL	0.105	2366	0.55
0.43	0.83	EB/SL	0.094	2134	0.56
0.35	2.48	SL	0.107	2413	0.53
0.44	1.66	SL	0.133	3016	0.54
2% Sand					
0.34	3.31	SL	0.111	2506	0.51
0.36	2.48	SL	0.107	2413	0.54
0.35	0.83	EB/SL	0.094	2134	0.56
0.42	2.48	SL	0.123	2784	0.54
0.42	1.66	SL/EB	0.119	2691	
3% Sand					
0.35	3.31	SL	0.113	2552	0.54
0.35	2.48	SL	0.101	2274	0.54

0.36	0.83	Mostly EB	0.082	1856	0.57
0.42	2.48	SL	0.123	2784	0.55
0.45	1.66	SL/EB	0.105	2366	0.58

Data used in dimensionless and regression analysis:

v_{SL} (m/s)	v_{SG} (m/s)	$(^{d_P}/_{d_L})$ (psi/ft)	$(^{d_P}/_{d_L})$ (Pa/m)	Flow Regime
Diesel Mix 2				
0.53	1.66	0.11	2552	SL
0.52	3.31	0.14	3248	SL
0.49	1.66	0.11	2413	SL
0.48	1.66	0.10	2320	SL
0.46	1.66	0.10	2227	SL
0.45	1.66	0.10	2181	SL
0.43	1.66	0.09	2042	SL
0.40	1.66	0.08	1902	SL
0.36	1.66	0.08	1763	SL
0.31	1.66	0.08	1902	SL
0.30	3.31	0.10	2366	SL
0.25	3.31	0.08	1763	SL
0.44	3.31	0.14	3155	SL
0.20	1.66	0.05	1234	SL
0.20	2.90	0.06	1392	SL
0.40	3.31	0.12	2784	SL
0.42	1.66	0.10	2227	SL
0.43	1.66	0.11	2506	SL
0.44	1.66	0.12	2645	SL
0.45	1.66	0.12	2691	SL
0.47	1.66	0.11	2598	SL
0.47	2.48	0.13	2970	SL
0.49	2.07	0.12	2784	SL
0.08	1.24	0.02	436	SL
0.08	2.07	0.02	557	SL
0.49	1.24	0.10	2320	SL
0.49	2.07	0.11	2543	SL
0.49	2.90	0.13	3016	SL

0.49	3.73	0.17	3944	SL
Diesel Mix 3				
0.21	1.24	0.06	1281	SL
0.21	1.66	0.06	1373	SL
0.31	1.66	0.09	1958	SL
0.31	3.31	0.10	2274	SL
0.26	0.83	0.07	1578	SL
0.25	1.24	0.07	1615	SL
0.25	3.31	0.09	1949	SL
0.35	1.66	0.09	2134	SL
0.35	2.07	0.10	2227	SL
0.35	2.69	0.11	2459	SL
0.38	1.86	0.11	2413	SL
0.38	2.48	0.12	2645	SL
0.42	1.66	0.12	2691	SL
0.42	2.48	0.13	2923	SL
0.45	1.86	0.12	2738	SL
0.44	1.66	0.12	2645	SL
0.42	1.66	0.11	2580	SL
0.39	1.66	0.10	2204	SL
0.35	1.66	0.09	2042	SL
0.41	2.48	0.11	2482	SL
0.35	2.48	0.10	2181	SL
Diesel Mix 3 + Sand				
0.45	1.86	0.13	2830	SL
0.45	2.48	0.14	3062	SL
0.45	3.31	0.14	3109	SL
0.31	1.66	0.10	2227	SL
0.35	1.66	0.10	2366	SL
0.35	2.07	0.11	2459	SL
0.25	3.31	0.08	1763	SL
0.27	3.31	0.07	1670	SL
0.35	3.31	0.11	2459	SL
0.41	2.48	0.12	2784	SL
0.41	1.66	0.12	2738	SL
0.42	3.31	0.14	3062	SL
0.39	1.66	0.10	2274	SL
0.28	2.48	0.07	1624	SL
0.20	2.90	0.06	1299	SL
0.20	1.66	0.06	1253	SL